X-ray emission from *z* pinches at 10^7 A: Current scaling, gap closure, and shot-to-shot fluctuations

W. A. Stygar, H. C. Ives, D. L. Fehl, M. E. Cuneo, M. G. Mazarakis, J. E. Bailey, G. R. Bennett, D. E. Bliss, G. A. Chandler, R. J. Leeper, M. K. Matzen, D. H. McDaniel, J. S. McGurn, J. L. McKenney, L. P. Mix, D. J. Muron, J. L. Porter, J. J. Ramirez, L. E. Ruggles, J. F. Seamen, W. W. Simpson, C. S. Speas, R. B. Spielman, K. W. Struve, J. A. Torres, and R. A. Vesey
Sandia National Laboratories, Albuquerque, New Mexico 87185-1196, USA

T. C. Wagoner, T. L. Gilliland, M. L. Horry, D. O. Jobe, S. E. Lazier, J. A. Mills, T. D. Mulville, J. H. Pyle, T. M. Romero, J. J. Seamen, and R. M. Smelser
Ktech Corporation, Albuquerque, New Mexico 87106-4265, USA
(Received 3 April 2003; published 14 April 2004)

We have measured the x-ray power and energy radiated by a tungsten-wire-array *z* pinch as a function of the peak pinch current and the width of the anode-cathode gap at the base of the pinch. The measurements were performed at 13- and 19-MA currents and 1-, 2-, 3-, and 4-mm gaps. The wire material, number of wires, wire-array diameter, wire-array length, wire-array-electrode design, normalized-pinch-current time history, implosion time, and diagnostic package were held constant for the experiments. To keep the implosion time constant, the mass of the array was increased as I^2 (i.e., the diameter of each wire was increased as I), where I is the peak pinch current. At 19 MA, the mass of the 300-wire 20-mm-diam 10-mm-length array was 5.9 mg. For the configuration studied, we find that to eliminate the effects of gap closure on the radiated energy, the width of the gap must be increased approximately as I. For shots unaffected by gap closure, we find that the peak radiated x-ray power $P_r \propto I^{1.24\pm0.18}$, the total radiated x-ray energy $E_r \propto I^{1.73\pm0.18}$, the x-ray-power rise time $\tau_r \propto I^{0.39\pm0.34}$, and the x-ray-power pulse width $\tau_w \propto I^{0.45\pm0.17}$. Calculations performed with a time-dependent model of an optically thick pinch at stagnation demonstrate that the internal energy and radiative opacity of the pinch are not responsible for the observed subquadratic power scaling. Heuristic wire-ablation arguments suggest that quadratic power scaling will be achieved if the implosion time τ_i is scaled as $I^{-1/3}$. The measured 1σ shot-to-shot fluctuations in P_r, E_r, τ_r, τ_w, and τ_i are approximately 12%, 9%, 26%, 9%, and 2%, respectively, assuming that the fluctuations are independent of I. These variations are for one-half of the pinch. If the half observed radiates in a manner that is statistically independent of the other half, the variations are a factor of $2^{1/2}$ less for the entire pinch. We calculate the effect that shot-to-shot fluctuations of a single pinch would have on the shot-success probability of the double-pinch inertial-confinement-fusion driver proposed by Hammer *et al.* [Phys. Plasmas **6**, 2129 (1999)]. We find that on a given shot, the probability that two independent pinches would radiate the same peak power to within a factor of $1\pm\alpha$ (where $0\leqslant\alpha\ll1$) is equal to $\mathrm{erf}(\alpha/2\sigma)$, where σ is the 1σ fractional variation of the peak power radiated by a single pinch. Assuming α must be $\leqslant7\%$ to achieve adequate odd-Legendre-mode radiation symmetry for thermonuclear-fusion experiments, σ must be $<3\%$ for the shot-success probability to be $\geqslant90\%$. The observed $(12/2^{1/2})\%=8.5\%$ fluctuation in P_r would provide adequate symmetry on 44% of the shots. We propose that three-dimensional radiative-magnetohydrodynamic simulations be performed to quantify the sensitivity of the x-ray emission to various initial conditions, and to determine whether an imploding *z* pinch is a spatiotemporal chaotic system.

DOI: 10.1103/PhysRevE.69.046403 PACS number(s): 52.58.Lq, 52.59.Qy, 52.25.Os, 52.80.Vp

I. INTRODUCTION

Wire-array *z* pinches are being developed as intense x-ray sources for inertial-confinement-fusion (ICF) experiments [1–118]. Several *z*-pinch-driven fusion concepts have been proposed and are being investigated [11,22,25,44,48, 49,52,55,63,76–78,87,88,96,100,108,110–112,114,118]. In the base-line approach, x-ray radiation from two colinear pinches drives a centrally located hohlraum that contains a thermonuclear-fusion fuel capsule [44,48,87,88,110–112,118]. This system, referred to as the *z*-pinch-driven hohlraum, requires that the x-ray power radiated by each pinch reach ~1200 TW, and that the total energy radiated per pinch exceed 8 MJ, to achieve a 400-MJ thermonuclear yield [44].

Radiation-symmetry requirements for this system are functions of the peak radiated x-ray power, total radiated x-ray energy, x-ray-power rise time, hohlraum-case-to-capsule ratio, capsule design, etc., and are still being determined [44,48,87,88,110–112,118]. Preliminary estimates indicate that, under the conditions described in Ref. [44], the peak powers radiated by the two pinches must differ by less than 7% to achieve the requisite odd-Legendre-mode capsule-drive symmetry. (Even-Legendre-mode symmetry is determined by the *z*-pinch, hohlraum and capsule geometries [18].) Consequently, development of a successful *z*-pinch-driven hohlraum requires not only that the x-ray-power and energy requirements be met, but that shot-to-shot fluctuations in the radiation emission be at or below acceptable levels.

Presently, wire-array pinches relevant to *z*-pinch-driven-hohlraum research radiate as much as 130 TW and 1.6 MJ of x rays from plasmas with 210-eV bright-

ness temperatures [24,35–37,67,87,88,102,110–112,118]. ICF experiments with ~100-ns pinch-implosion times are being conducted at 17–19-MA [24,35–37,67,87,88,110–112,118] on the Z accelerator [119–127]. Higher-current machines are being proposed to increase the radiated power and energy [128,129].

To optimize the design of the next generation of accelerators, it is necessary to understand how the radiation emission from a pinch, and the statistical fluctuations in the emission, vary with the peak pinch current I. It is usually assumed that both the peak radiated x-ray power and total radiated x-ray energy are proportional to I^2. These are the two most important and fundamental z-pinch-physics assumptions made when projecting the performance of future higher-current accelerators. However, it appears that the precise origins and validity of these two assumptions are not well defined and must be reexamined.

The notion that the radiated power and energy scale as I^2 stems, in part, from arguments similar to the following. We consider a wire-array z pinch and model the array as an infinitely thin perfectly stable cylindrical foil. When such a foil carries current and as a result accelerates inward toward its axis of symmetry, the kinetic energy of the foil increases as the foil radius decreases. When the foil stagnates upon itself on axis, the foil's kinetic energy is thermalized and subsequently radiated as x rays [1].

For such an imploding-foil z pinch, we have the following:

$$\frac{\mu_0 \ell I^2 f^2(t)}{4\pi} = -mr(t)\frac{d^2 r}{dt^2}(t), \tag{1}$$

$$\tau_i \equiv \int_b^a \frac{dr}{v(r)}, \tag{2}$$

$$E_k(r) \equiv \frac{1}{2} m v^2(r) = \frac{-\mu_0 \ell I^2}{4\pi} \int_b^r \frac{F^2(r)dr}{r}, \tag{3}$$

where μ_0 is the free-space magnetic permeability, ℓ is the axial length of the pinch, I is the peak pinch current, $f(t)$ is the normalized pinch current as a function of time, m is the pinch mass, $r(t)$ is the pinch radius as a function of time, τ_i is the pinch-implosion time, b is the initial pinch radius, a is the final pinch radius, $v(r)$ is the pinch velocity as a function of r, $E_k(r)$ is the pinch kinetic energy as a function of r, and $F(r)$ is the normalized pinch current as a function of r, where $F(r(t)) \equiv f(t)$. (Equations are in SI units throughout.) We define a to be the effective radius at which the pinch stagnates and its kinetic energy is thermalized.

If ℓ, a, b, and $F(r)$ do not change as I is increased, then the peak pinch kinetic energy $E_k(a)$ is proportional to I^2. If the fraction of $E_k(a)$ that is thermalized and radiated as x rays is independent of I, then the total radiated x-ray energy is proportional to I^2. If in addition the time constants associated with the thermalization of $E_k(a)$ and subsequent radiation emission are independent of I, then the peak radiated x-ray power is also proportional to I^2.

The above arguments, however, do not consider one-, two-, and three-dimensional effects, instabilities, wire-ablation processes [8,9,10,12,17,19,31,32,39,47,57,58,60,68,74,80,85,86,91,92,98,109,113,116], parasitic currents [17], PdV work performed on the pinch plasma after stagnation [27], etc. Hence it is not clear that the total radiated x-ray energy and peak radiated x-ray power are always proportional to I^2.

It has been reported in the literature that the measured radiated x-ray *energy* $\propto I^2$ [22,49,101]. The I^2-scaling data presented in [22,49,101], however, were not obtained in a controlled manner. The data presented are that obtained from pinches that were *optimized* for each accelerator. The four measurements presented in [22,49,101] were obtained on the Supermite, Proto-II, Saturn, and Z accelerators, each of which produced a different normalized-pinch-current time history. In addition, although the axial length of the pinch was held constant, other critical pinch parameters, such as the pinch material, initial pinch diameter, pinch electrode configuration, and implosion time, were changed to optimize the radiated energy. Specifically, the Supermite and Proto-II data were taken with argon gas-puff z-pinches; the Saturn and Z data were taken with tungsten wire-array z pinches. The Saturn and Z data were taken with wire-array diameters that differed by more than a factor of 2. The implosion times for these four accelerators ranged from ~50 to ~100 ns; the accelerator-circuit designs were also significantly different. Consequently, the I^2-scaling data presented in [22,49,101] have a significant spread in pinch parameters and are not entirely physically meaningful.

Moreover, recently reported Saturn measurements suggest that I^2 energy scaling has, in fact, *not* been demonstrated between optimized pinches on Saturn and Z, presently two of the world's most powerful z-pinch drivers. The highest yield achieved on Saturn at 6.4 MA is 0.53 MJ [20]; at 7.6 MA the highest yield is 0.8 MJ [40]. These yields are to be compared with the 1.9 MJ that has been achieved on Z at 19 MA [34], which is less than the 4.7–5.0 MJ expected assuming I^2 scaling from the Saturn results.

Furthermore, even though it is commonly assumed that the peak radiated x-ray *power* $\propto I^2$, no data have been presented that support this assumption. In fact, recent measurements indicate that I^2 power scaling has *not* been demonstrated between optimized pinches on Saturn and Z. The highest x-ray power achieved on Saturn at 8 MA using an optimized pinch is 75 TW [20]; the highest power achieved on Z at 19 MA is 230 TW [26]. The 230 TW is less than the 420 TW expected, assuming I^2 scaling from the Saturn result. Hence I^2 scaling for neither energy nor power has been demonstrated for *optimized* pinches between Saturn and Z.

The physics of current scaling might be better explored through examination of the results of *controlled* scaling experiments; it appears, however, that the literature does not describe such results. Information on shot-to-shot fluctuations in the radiation emission from pinches also appears to be incomplete. In addition, to optimize the design of the next-generation accelerators, it is important to understand how the x-ray emission from a pinch varies with the anode-cathode gap of the vacuum transmission line that delivers

electromagnetic power to the pinch. The literature, however, contains little discussion of the effects of gap closure on the x-ray emission.

In this paper, we present *controlled* measurements of the peak radiated x-ray power, total radiated x-ray energy, x-ray-power rise time, and x-ray-power pulse width as functions of the peak pinch current and the width of the anode-cathode gap at the base of the pinch. We also present measurements of statistical fluctuations in the power, energy, rise time, pulse width, and pinch-implosion time as functions of current. The experiments were conducted on the Z accelerator, the highest-current 10^{-7}-s pulse generator developed to date [119–127]. The pinch configuration used is the tungsten-wire-array design first characterized by Deeney and Spielman [130], Porter [24], and Baker *et al.* [35–37,67], and is the base line presently being developed as the driver for *z*-pinch-driven hohlraum experiments [87,88,110–112,118].

The experimental arrangement is described in Sec. II. Measurements of the x-ray power, energy, rise time, and pulse width as functions of the peak pinch current and anode-cathode gap are presented in Sec. III A. In Sec. III B, we develop a time-dependent model of an idealized optically thick pinch at stagnation, and demonstrate that the observed subquadratic x-ray-power scaling is not due to radiation trapping or the energy sink represented by the pinch's internal energy. We discuss the implications of the observed power scaling in Sec. III C 1. In Sec. III C 2, we develop heuristic scaling relations for the wire array described in Sec. II. The relations suggest that the x-ray-power scaling will improve if the pinch implosion time τ_i is decreased as I is increased. In Sec. III C 3, we speculate that *predictive* three-dimensional radiative-magnetohydrodynamic (MHD) simulations might ultimately be required to design an optimized pinch-accelerator system.

Measurements of shot-to-shot fluctuations in the power, energy, rise time, pulse width, and implosion time as functions of the peak pinch current are presented in Sec. IV A. We also present images of the pinch (recorded with an x-ray framing camera) that show significant shot-to-shot variations in the spatial structure of the x-ray emission. The radiation measurements described in Secs. III A and IV A (except those made with the camera) were performed on one-half of the pinch. The inference of shot-to-shot fluctuations for the entire pinch from these measurements is discussed in the Appendix. In Sec. IV B, we estimate the effect that random fluctuations in the radiation emission from a single pinch would have on the shot-success probability of the double-pinch ICF driver. In Sec. IV C, we briefly describe two-dimensional MHD simulations that are in qualitative agreement with the observed fluctuations in the radiation emission. We also propose that a systematic computational study be initiated to quantify the source and nature of the apparently random fluctuations, and to determine whether the evolution (in time and space) of a *z* pinch is chaotic.

II. EXPERIMENTAL ARRANGEMENT

The experiments described below were conducted on the Z pulsed-power accelerator, the highest-current 10^{-7}-s pulse generator developed to date [119–127]. The results of 17 accelerator shots are described: 6 shots were taken with a 13-MA peak pinch current; 11 shots were taken at 19 MA. On each of these shots, the current pulse drove the implosion of a single tungsten-wire-array *z* pinch. The higher peak current is the most that could routinely be delivered to the pinch. The lower was achieved by reducing the Z-accelerator Marx-charge voltage, gas-switch pressures, and water-switch gaps [131]. As indicated in Fig. 1, these changes were made in a manner that kept the shape of the Z forward-going-voltage pulse (which ultimately drove the pinch implosion) the same at 13 and 19 MA. The normalized standard deviation of the pointwise difference between the shapes of the forward-going pulses at 13 and 19 MA is less than 2%. (The pointwise difference between the normalized pinch currents at 13 and 19 MA is also less than 2%, as discussed in Sec. III C 2.)

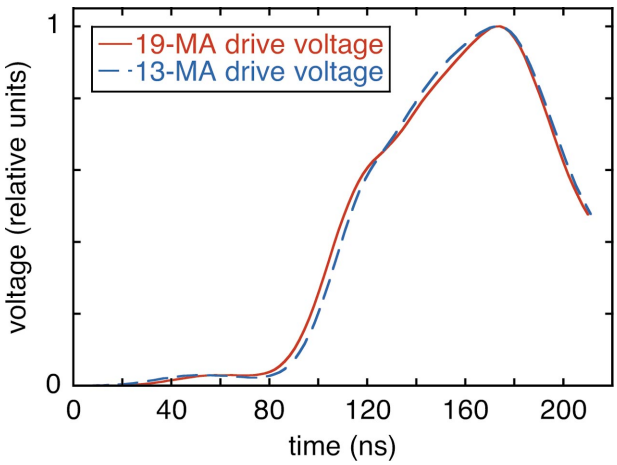

FIG. 1. (Color) Normalized Z-accelerator forward-going voltages for the 13- and 19-MA peak-current shots. The 13-MA drive voltage is an average of the voltages measured on the six 13-MA shots; the 19-MA voltage is an average of the voltages measured on the eleven 19-MA shots. The normalized standard deviation of the pointwise difference between the two pulses is less than 2%.

The wire-array design used for the experiments is outlined in Fig. 2. The wire material, number of wires, wire-array diameter, wire-array length, wire-array electrode design, normalized-pinch-current time history, implosion time, and

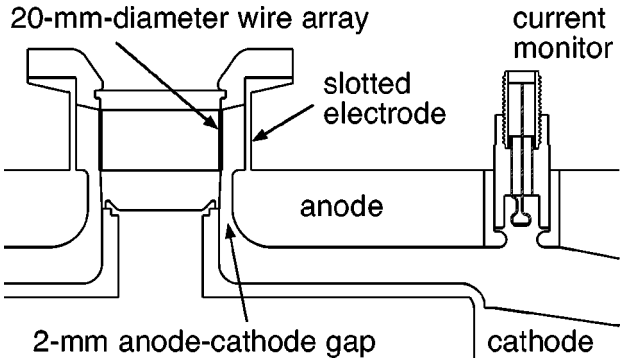

FIG. 2. Schematic of the wire-array geometry. (Drawing is to scale.)

diagnostic package were held constant for all of the shots taken at both 13 and 19 MA. Since we held the pinch geometry and implosion time constant, we also held the *nominal* inter-wire-gap, time-dependent implosion velocity, time-dependent pinch inductance, and number of Rayleigh-Taylor growth periods [21] constant.

To keep the implosion time τ_i constant, we increased the mass of the array m as I^2; i.e., the diameter of each wire was increased as I. This is the most straightforward possible controlled current-scaling experiment, assuming the zero-dimensional pinch model given by Eqs. (1)–(3). These equations predict that when m is increased as I^2 and ℓ, b, and $f(t)$ are held constant as I is increased, then $E_k(r) \propto I^2$, and $r(t)$, $v(r)$, $F(r)$, and τ_i also remain constant. (τ_i is, for all practical purposes, independent of a when $a \ll b$.)

Equations (1)–(3) predict that when $a \ll b$, the peak kinetic energy $E_k(a)$ is a weak function of a. We do not, however, have direct control over the value of a or how a changes with I. Consequently, for the experiments, we increased m as I^2 and held ℓ, b, and $f(t)$ constant for all of the shots to determine *under these conditions* how the radiation emission varies with current. This is not only the most straightforward but also the most relevant possible scaling experiment, since this scaling is that which is presently being assumed for the design of future higher-current z-pinch accelerators.

The circular tungsten-wire array (Fig. 2) had a 10-mm axial length, a 20-mm diameter, and consisted of 300 equally spaced tungsten wires. The array was contained within a slotted cylindrical electrode. The radial gap between the wires and the inside surface of the slotted electrode was held constant at 4 mm. The electrode had 9 equally spaced 5.6-mm-wide slots that provided diagnostic access to the pinch. The radial gap at the base of the array is shown as 2 mm in Fig. 2, and was varied from 1 to 4 mm.

The anode and cathode electrodes of the wire array, and the vacuum transmission line (outlined in Fig. 2) that delivered electromagnetic power to the pinch, were made of stainless steel and were machined to a finish with a root-mean-square roughness of less than 0.41 μm. After machining, the electrodes were mechanically scrubbed with a mild alkaline detergent, electropolished, mechanically scrubbed again, hydrogen fired, and vacuum baked. The power-flow surfaces of the wire-array electrodes (except for the slotted electrode) were subsequently coated with 10 μm of gold; the transmission-line electrodes were coated with 3 μm. (The slotted electrode was not coated.) The experiments were conducted at nominal pressures that ranged from 0.3×10^{-5} to 1.8×10^{-5} torr (from 0.4×10^{-3} to 2.4×10^{-3} Pa).

A modified version of the original 20-mm-diam tungsten-wire-array design was developed for these experiments. In the original design, the gap between the wires and slotted electrode was 2.5 mm, and the slots introduced a $\pm30\%$ azimuthal variation in B^2 at the wires (where B is the absolute value of the magnetic field). In the modified design used for the experiments, the gap between the wires and slotted electrode was 4 mm (as indicated in Fig. 2), which decreased the azimuthal variation in B^2 to $\pm10\%$. The modified design also reduced azimuthal variations (due to fabrication tolerances) in the anode-cathode gap at the base of the pinch from ±0.23 mm to ±0.09 mm, and variations in the diameter of the upper and lower 20-mm-diam wire-array electrodes from ±0.025 mm to ±0.013 mm. These changes improved the concentricity of the wire-array hardware and reproducibility of the implosion time. The modified design also improved the current contacts between the wires and upper and lower wire-array electrodes. The design was used on all of the shots except 566; on this shot, the anode-cathode gap between the wires and slotted electrode was 4 mm, but the fabrication tolerances and current contacts were those of the original design.

Although the wire-array hardware was fabricated with tolerances controlled more carefully than for any previous wire-array experiment, there nevertheless remained potential sources of shot-to-shot fluctuations that were not addressed. For example, the wire-array mass m was determined by measuring 1% of the wire used to fabricate the array. This may have allowed more variation in m and therefore the implosion time τ_i than desired. Also, although the *nominal* inter-wire gap was held fixed at 209 μm, the *actual* wire-to-wire gaps exhibited random variations of $\pm(8-12)\%$ [88]. The 7.7- and 11.4-μm-diam wires (used on the 13- and 19-MA shots, respectively) were located in $\sim$70-μm-wide slots that were electric-wire-discharge machined in the wire-array-electrode hardware. In addition, the wires exhibited random variations in angle with respect to vertical on the order of $\pm(0.5°-1°)$. Effects on the x-ray-power rise time from deliberate inter-wire-spacing perturbations resulting from the manner in which the wires were positioned and tensioned have been noted at the 30% level [88]. Recent confirmation on Z of delayed wirelike implosion trajectories for these wire arrays [132] suggest that array performance may be sensitively dependent on small-scale azimuthal variations in the wire locations. (We note that an interesting discussion of the effects of large-scale symmetry-breaking perturbations on the x-ray emission is presented by Marder, Sanford, and Allshouse in Ref. [32].)

Both x-ray and electrical diagnostics were fielded on each shot. The x-ray-diagnostic package included a five-channel x-ray-diode (XRD) array [133], two nickel bolometers (which were used to integrate the radiated power over a $\sim$40-ns time interval) [134], a calorimeter (which was used to integrate over a $\sim$2-ms interval) [135], and a microchannel-plate x-ray framing camera [136,137]. The pinch power was determined by normalizing a spectrally equalized linear combination of the five XRD signals to the average of the two bolometer energy measurements [138]. The x-ray powers and energies inferred from the measurements assume that the pinch was a Lambertian emitter for both the 13- and 19-MA peak-current shots. The x-ray diagnostics (except for the x-ray camera) viewed one-half of the pinch at a 12° angle above the pinch's equatorial plane. The camera observed almost the entire height of the pinch and was filtered with 4.8 μm of Kimfol and 0.13 μm of aluminum.

The electrical-diagnostic package included two recessed magnetic-flux (dB/dt) monitors that measured the Z-accelerator load current 6 cm from the axis of the pinch.

TABLE I. Summary of the experimental results. The gap-closure time is relative to peak x-ray power.

Z shot number	Peak pinch current I (MA)	Anode-cathode gap (mm)	Peak x-ray power P_r (TW)	Bolometer x-ray energy E_r (MJ)	Calorimeter x-ray energy E_r (MJ)	X-ray-power rise time τ_r (ns)	X-ray-power pulse width τ_w (ns)	Pinch-implosion time τ_i (ns)	Gap-closure time (ns)	Total pinch mass m (mg)
648	12.9	1	84	0.66	0.73	3.5	7.8	94	−1.4	2.64
820	13.1	1	92	0.63	0.79	3.1	6.9	95	−1.8	2.72
649	12.9	2	85	0.85	0.97	3.7	10.0	94		2.63
647	12.6	3	69	0.81	0.92	5.3	11.6	96		2.62
725	13.0	4	73	0.76	0.99	5.4	10.4	93		2.74
819	12.7	4	89	0.86	1.09	5.3	9.7	96		2.74
646	19.2	1	88	0.92	1.16	5.0	10.4	96	−1.5	5.85
684	18.6	1	112	1.07	1.17	4.2	9.6	94	5.3	5.85
566	19.3	2	142	1.28		3.8	9.0	97		5.89
597	19.5	2	137	1.30	1.45	4.7	9.5	95		5.86
682	19.3	2	84	1.04	1.09	4.5	12.4	93		5.91
594	18.8	3	120	1.50	1.74	5.5	12.5	94		5.85
683	18.1	3	135	1.55	1.65	4.4	11.5	96		5.85
723	18.3	4	121	1.53	1.84	5.0	12.6	95		5.91
724	19.1	4	153	1.76	2.00	5.5	11.5	95		5.87
817	18.2	4	92	1.28	1.52	8.1	13.9	96		5.85
818	18.6	4	143	1.70	1.97	4.5	11.9	97		5.87

(We define the load to be all of the hardware located inside a 6-cm radius; hence the load includes the wire-array pinch.) The load monitors were fielded 150° apart; one such monitor is shown in Fig. 2. On shots taken with a peak current of 13 MA, we used these current measurements, and electrical measurements made in the Z magnetically insulated transmission lines (MITL's) and insulator stack [139], to normalize a circuit model of Z. The load-current measurements at 19 MA were increased by 2% to be consistent with the other electrical measurements on these shots, as indicated by the circuit model. (We believe that the load-current measurements were slightly more accurate at 13 than at 19 MA, because the monitors were more damaged by MITL flow electrons [140–143] at the higher current.)

The magnetic field in the anode-cathode gap at the base of the pinch was 260 and 380 T at 13 and 19 MA, respectively. According to circuit simulations with an infinitely thin perfectly stable cylindrical-foil-pinch model [Eqs. (1)–(3)] and a 10:1 pinch-radius convergence ratio, the mean electric field in the gap (when it was 1 mm) reached ~50 and ~70 MV/cm on the 13- and 19-MA peak-current shots. (We note that the configuration outlined in Fig. 2 can serve as a laboratory source of high magnetic and electric fields for atomic-physics research.) The simulations suggest that the electric field increased rapidly as a function of time near the end of the implosion and peaked immediately before the pinch stagnated on axis. Using the z-pinch-driven hohlraum model given by Eq. (41) of Ref. [102], we estimate that the temperature of the surface of the gap electrodes peaked at ~90 and ~100 eV for the 13- and 19-MA shots, when the x-ray power radiated by the pinch reached its maximum value.

III. CURRENT SCALING AND GAP CLOSURE

A. Measurements

Measurements of the peak radiated x-ray power P_r, the total radiated x-ray energy E_r, the 10%–90% x-ray-power rise time τ_r, and the effective x-ray-power pulse width $\tau_w \equiv E_r/P_r$ as functions of the peak pinch (load) current I and the anode-cathode gap at the base of the pinch are presented in Table I and Figs. 3–9.

Figures 3 and 4 plot P_r and E_r as functions of the current and gap. The error bars in Figs. 3 and 4 are standard deviations estimated from the shot-to-shot fluctuations represented in Figs. 7 and 8, respectively, and assume these fluctuations are independent of I. (A more detailed discussion of shot-to-shot fluctuations is presented in Sec. IV and the Appendix.)

It appears that the x-ray power and energy are more affected by gap closure at the higher current. (For this discussion, we define gap closure to be a decrease in the impedance of the gap.) For the system oultined in Fig. 2, the voltage across the gap as a function of time $V(t)$ is approximately $d[L(t)I(t)]/dt$, where $L(t)$ and $I(t)$ are the pinch inductance and current as a function of time, respectively. When the nominal pinch inductance and implosion time are held constant, as they were for the experiments, $V(t)$ scales approximately as $I(t)$. Under these conditions, the ratio $V(t)/I(t)$ is independent of the peak pinch current I. Since the results presented in Figs. 3 and 4 imply that at constant initial gap, the fractional current lost across the gap increases with increasing I, it appears that the effective gap impedance decreases as I is increased.

Time-resolved current and x-ray-power measurements are presented in Figs. 5 and 6. As indicated in these figures, the

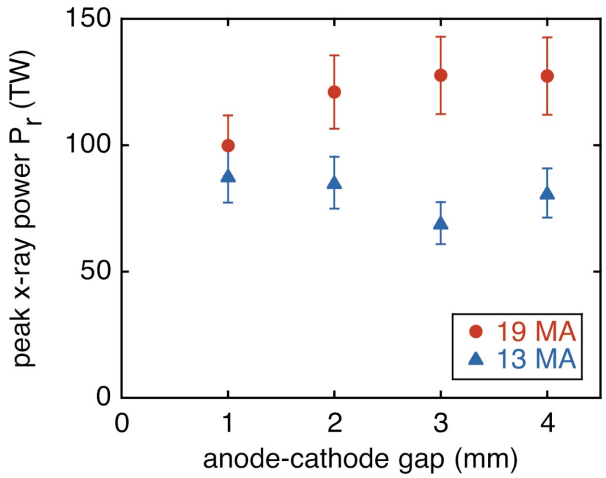

FIG. 3. (Color) Measurements of the peak radiated x-ray power P_r as a function of anode-cathode gap and peak pinch current. The standard deviation due to shot-to-shot fluctuations is estimated from the data to be 12%, assuming the fluctuations are independent of current.

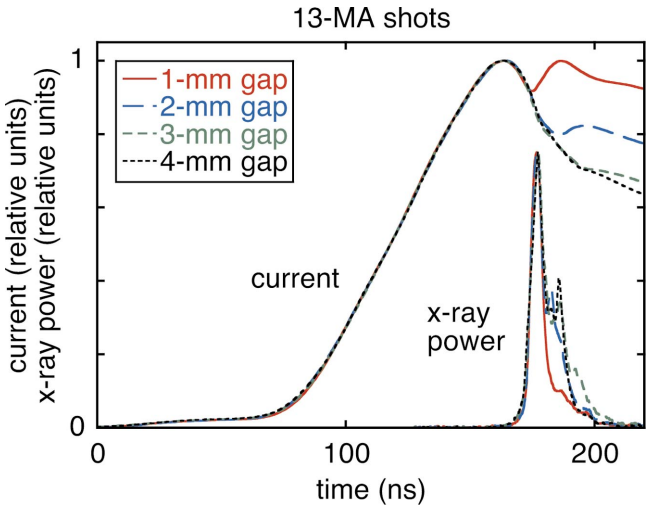

FIG. 5. (Color) Time-resolved measurements of the current and x-ray power as a function of anode-cathode gap for shots 648, 649, 647, and 725, which were taken with a 13-MA peak pinch current. The traces have been normalized and time shifted to facilitate comparisons of the current and x-ray-power time histories.

decrease in the radiated energy as the gap decreases is accompanied by a reduction in the tail of the x-ray-power pulse. (As indicated in Table I, P_r also decreases as the gap is decreased.) The 1-mm-gap current wave forms in Figs. 5 and 6 show evidence of an abrupt decrease in the load inductance due to gap closure during the radiation pulse. Apparent closure times relative to the peak of the x-ray power for these 1-mm-gap shots are listed in Table I.

We note that the 1- and 2-mm-gap 13-MA current wave forms of Fig. 5 show clearer evidence of gap closure than the corresponding 19-MA wave forms of Fig. 6. This observation and those made previously suggest that there may be two mechanisms for current loss across the gap: (1) a loss that begins before peak x-ray power, which Figs. 3 and 4 suggest increases as I is *increased*, and (2) an abrupt loss that begins near peak x-ray power, which becomes more severe as I is *decreased*, as indicated by the 1- and 2-mm-gap wave forms in Figs. 5 and 6. The observation that the second mechanism becomes more severe as I is decreased might be consistent with the gap-closure model described by Cuneo *et al.* [87]. We caution, however, that the load-current monitors become less accurate after peak current as I is increased, as discussed in Sec. III C 2.

It appears that larger gaps will be needed as the current is increased in future accelerators if identical electrode designs, electrode treatment, and materials are used, and if the design of the MITL's is the same as that presently being fielded on the Z accelerator [120,122,127]. (When the MITL design is

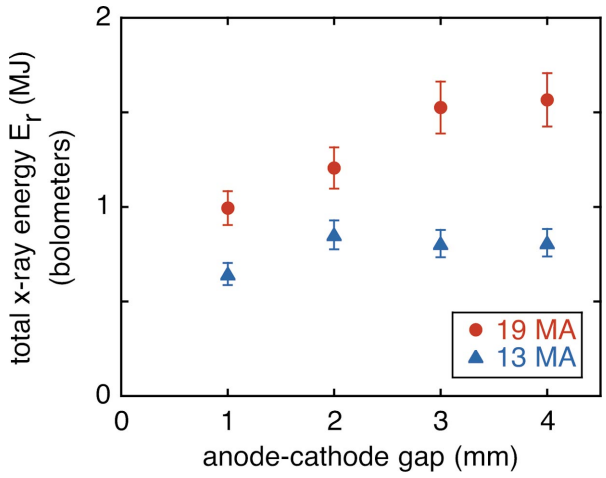

FIG. 4. (Color) Measurements of the total radiated x-ray energy E_r inferred from the bolometers as a function of anode-cathode gap and peak pinch current. The standard deviation due to shot-to-shot fluctuations is estimated from the data to be 9%, assuming the fluctuations are independent of current.

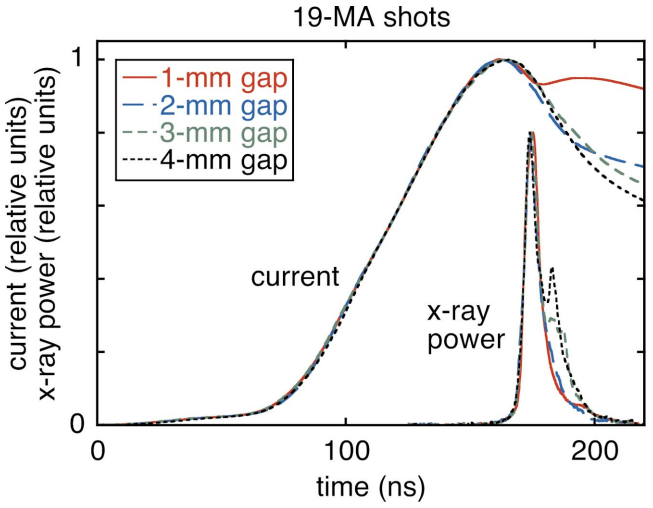

FIG. 6. (Color) Time-resolved measurements of the current and x-ray power as a function of anode-cathode gap for shots 684, 597, 683, and 818, which were taken with a 19-MA peak pinch current. The traces have been normalized and time shifted to facilitate comparisons of the current and x-ray-power time histories.

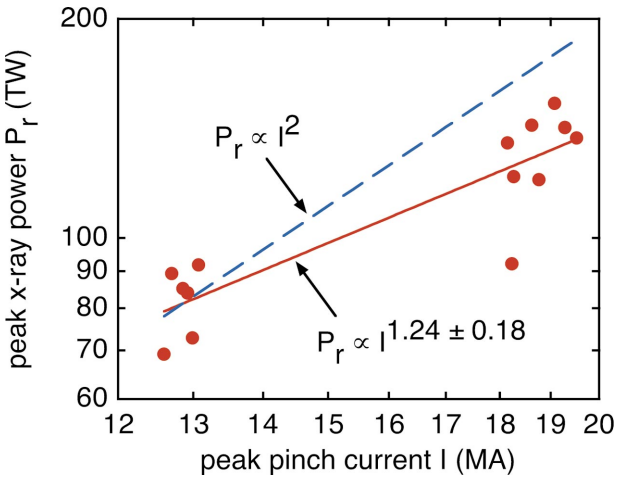

FIG. 7. (Color) Measurements of the peak radiated x-ray power P_r as a function of the peak pinch current I, for shots unaffected by gap closure.

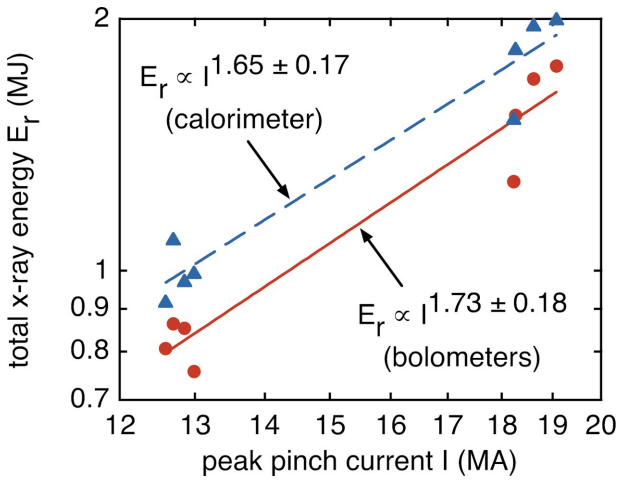

FIG. 8. (Color) Measurements of the total radiated x-ray energy E_r as a function of the peak pinch current I, for shots unaffected by gap closure.

held constant, as it was for the experiments, the electron-flow current launched in the MITL's [120,122,127,140–143] increases approximately with I. When the peak current was increased from 13 to 19 MA in the experiments, the corresponding increase in the flow current contributed to the decrease in the gap impedance, although it is presently unknown to what extent.)

We estimate from the data presented in Fig. 4 that the minimum gap required for E_r to be unaffected by gap closure is, to zeroth order, proportional to I. For example, for the wire array outlined in Fig. 2, a ~4.7-mm gap will be needed for shots taken with $I=30$ MA. Assuming, as suggested by Fig. 3, that a ~1.5-mm gap is required at 19 MA for P_r to be unaffected by gap closure, and that this minimum gap is also proportional to I, we estimate that a ~2.4-mm gap will be required at 30 MA. Preliminary *double*-pinch experiments are being performed on Z [110–112,118] at 17 MA, with a 3-mm gap to optimize the radiation emission from the two pinches. (The double-pinch system described in [110–112,118] produces, at the gap, 2–3 times the electric field of the single-pinch system described in Sec. II.) We estimate that to achieve the same relative radiation emission with the double-pinch configuration at 30 MA as at 17 MA would require a 5.3-mm gap.

Figures 7–9 plot P_r, E_r, τ_r, and τ_w as functions of I. To isolate just the effect of current scaling on the x-ray production, we use for these figures only measurements that appear to be unaffected by gap closure: for Fig. 7 and the plot of $\tau_r=\tau_r(I)$ in Fig. 9, we use all of the shots except 646, 682, and 684; for Fig. 8 and the plot of $\tau_w=\tau_w(I)$ in Fig. 9, we use shots 647, 649, 723–725, and 817–819.

The results presented in Figs. 7–9 can be summarized as follows:

$$P_r \propto I^{1.24 \pm 0.18}, \tag{4}$$

$$E_r \propto I^{1.73 \pm 0.18}, \tag{5}$$

$$\tau_r \propto I^{0.39 \pm 0.34}, \tag{6}$$

$$\tau_w \propto I^{0.45 \pm 0.17}. \tag{7}$$

Equation (5) is obtained from the bolometer data and is essentially equivalent to the scaling observed with the calorimeter. As discussed above, these relations apply when P_r, E_r, τ_r, and τ_w are unaffected by gap closure. The uncertainty given in each of these equations is the 1σ value estimated from a least-squares fit to a power law. It appears that for the conditions studied, neither P_r nor E_r scales as I^2, and that τ_r and τ_w are increasing functions of I.

B. Model of an optically thick pinch at stagnation

As described above, we increased m as I^2 to keep τ_i constant. Hence the internal energy and radiative opacity of the pinch were increased substantially as the peak pinch current was increased. In this section, we estimate under these conditions to what extent the internal energy and opacity

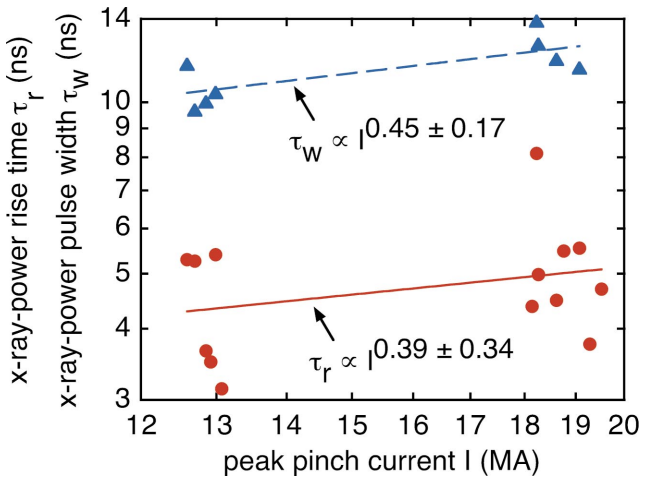

FIG. 9. (Color) Measurements of the 10%–90% x-ray-power rise time τ_r and effective x-ray-power pulse width $\tau_w \equiv E_r/P_r$ as functions of the peak pinch current I, for shots unaffected by gap closure.

affect the scaling of P_r, τ_r, and τ_w with current. For these calculations, we make the simplifying assumption that $E_r \propto I^2$.

Extending results presented in [87,102], we develop below a time-dependent model of an optically thick tungsten *z* pinch at stagnation. We idealize the pinch as a cylinder with a radius that, over the time interval of interest, remains constant [87,102]. Assuming that power is conserved and that the pinch electrons, ions, and radiation field are at the same temperature, we write [102,144]

$$\frac{dU}{dt} = P_{th} - A\sigma_{SB}T_b^4, \tag{8}$$

$$U = \frac{3}{2}NZk_BT_{ave} + N\sum_{j=1}^{Z} I_j + \frac{4}{c}V\sigma_{SB}T_{ave}^4, \tag{9}$$

$$Z \sim 0.02(T_{ave}^{1/2}), \tag{10}$$

$$\sum_{j=1}^{Z} I_j \equiv ZI_{ave} \sim 2Zk_BT_{ave}, \tag{11}$$

where U is the pinch's internal energy [144], P_{th} is the total thermal power delivered to the pinch, A is the pinch surface area, σ_{SB} is the Stefan-Boltzmann constant, T_b is the pinch brightness temperature, N is the number of tungsten ions in the pinch, Z is the tungsten ionization charge state, k_B is the Boltzmann constant, T_{ave} is the average pinch temperature, I_j is the jth ionization potential of tungsten, V is the pinch volume, c is the speed of light, and I_{ave} is the average of the first Z ionization potentials. The expression for U [Eq. (9)] neglects the ion thermal energy, which is valid when $Z \gg 1$. Equation (9) also neglects the energy of excited electronic states, the energy of the electric and magnetic fields, and the decrease in U due to the Coulomb-interaction energy between the charged particles [144].

We supplement Eqs. (8)–(11) with the following simplifying assumptions:

$$P_{th} = P_0 \sin^2\left(\frac{t}{\tau_{th}}\right), \tag{12}$$

$$P_0 \equiv C\left(\frac{I}{I_0}\right)^2, \tag{13}$$

$$N = N_0\left(\frac{I}{I_0}\right)^2, \tag{14}$$

where τ_{th} is the thermalization time constant—i.e., the characteristic time over which the energy made available to the pinch is thermalized. We normalize Eqs. (12)–(14) to the experiments conducted at 13 MA: we set the constants I_0 and N_0 to 13 MA and 9×10^{18}, respectively, and adjust the constants C and τ_{th} to obtain the measured values of E_r and P_r at 13 MA. As implied by Eqs. (12) and (13), we assume for these calculations that the total radiated energy E_r (which equals $\pi\tau_{th}P_0/2$) is proportional to I^2.

We also assume that either the pinch is isothermal [102],

$$T_{ave} = T_b, \tag{15}$$

or that [87]

$$T_{ave} = 0.7\left(\frac{a}{\lambda}\right)^{1/4} T_b, \tag{16}$$

$$\lambda = \frac{1.06\times10^{-11}}{K_0\rho^{1.3}} T_{ave}^{3/2}, \tag{17}$$

where a is the pinch radius, λ is the Rosseland mean free path (as given in [145]), K_0 is an opacity multiplier, and ρ is the pinch mass density. Equation (15) applies when the pinch temperature is independent of radius, which would be applicable when there is sufficient turbulent mixing of the core with the outer regions of the pinch [44]. Equation (16) applies when the pinch-temperature distribution is given by the one-dimensional steady-state radiation-diffusion equation, and the thermal power source is independent of radius [87]. (When turbulent mixing and other forms of convection can be ignored, we estimate that the steady-state profile is a good approximation near peak x-ray power.) Equation (16) also assumes that $a/\lambda > 5$ [87]. For the conditions described above, we find that $a/\lambda > 7$ for peak pinch currents $\geqslant 13$ MA.

We assume $a = 1$ mm, which we estimate from images of the pinch recorded with the x-ray camera. Three sets of calculations were performed: for $T_{ave} = T_b$, $T_{ave} \neq T_b$ and $K_0 = 1$, and $T_{ave} \neq T_b$ and $K_0 = 2$. The equations were solved numerically. The numerical energy-conservation error at peak x-ray power when $I = 60$ MA is less than 1 part in 10^6. Results are presented in Figs. 10 and 11.

For all three calculations, the peak x-ray power $P_r \propto I^{2.00}$ between 13 to 19 MA (Fig. 10). (Between 19 and 60 MA, the power-scaling exponents are 2.00, 1.97, and 1.94 for the three cases, respectively.) The calculated rise times decrease between 13 and 19 MA (Fig. 11), and the calculated pulse widths are constant to within less than one percent. Hence it appears that the internal energy and radiative opacity of the pinch as modeled above cannot account for the observed subquadratic P_r scaling, and the observed increase of τ_r and τ_w with I.

If we assume in our calculations that P_0 is proportional to $I^{1.73}$,—i.e., that the total radiated energy $E_r \propto I^{1.73}$ (as observed experimentally)—we must also assume that the thermalization time constant τ_{th} increases approximately as $I^{1/2}$ (i.e., as $m^{1/4}$) to reproduce the measured power scaling. In other words, the observed power scaling would be consistent with a thermalization process that lengthens in duration as I (and m) are increased.

C. Discussion

1. Motivation for improving the power scaling

For the experiments described in Sec. III A, the measured peak x-ray power at 13 MA is ~80 TW (Fig. 7). Assuming that the power could be made to scale as I^2 for peak currents greater than 13 MA, the peak power at 50 MA would be 1200 TW. This is the power required per pinch to achieve a

400-MJ thermonuclear yield with the z-pinch-driven hohlraum [44]. Assuming instead that $P_r \propto I^{1.24}$ for currents greater than 13 MA, we estimate that ~115 MA would be required to achieve 1200 TW. (Of course, we only measured the scaling between 13 and 19 MA and do not know how the power scales for currents greater than 19 MA.) Since the difference in size and cost between 50- and 115-MA accelerators is a factor of 5, it is of interest to understand the subquadratic power-scaling results presented in Sec. III A and to attempt to achieve I^2 scaling for currents greater than 13 MA.

2. Heuristic scaling relations

Following arguments developed by Yadlowski *et al.* [17], Chittenden and co-workers [68], and Cuneo *et al.* [132,146], we propose that effects due to wire ablation [8,9,10, 12,17,19,31,32,39,47,57,58,60,68,74,80,85,86,91,92,98,109, 113,116] be investigated as possible contributors to the results presented in Sec. III A. These arguments are consistent with recent experiments conducted on the Z accelerator [132], which have shown the existence of a plasma precursor and an array-implosion trajectory delayed [from that predicted by the imploding-foil model, Eqs. (1)–(3)] due to wire-ablation effects.

When the peak current delivered to a wire-array z pinch is increased, the wire-mass density, number of wires, wire-array diameter, diameter of each individual wire, normalized pinch current time history, and implosion time cannot simultaneously be held constant. Hence the wire-ablation process must change as the peak current I is changed. For example, if the wire-mass density, number of wires, wire-array diameter, normalized pinch-current time history, and implosion time are held constant as I is increased (as they were for the experimental arrangement described in Sec. II), then the diameter of each individual wire must be increased as I. In such a system, at very early times in the current pulse, the current density in each wire is proportional to I^{-1}, and the initial heating rate of the wires is proportional to I^{-2}.

A complete understanding of wire ablation and current scaling will likely require a systematic set of numerical r-θ-z wire-array simulations as a function of I and other critical wire-array parameters. It might be useful, however, to consider the following heuristic scaling relations for the wire array described in Sec. II.

For the discussion below, we assume that the wire-mass density, number of wires, wire-array diameter, and wire-array length are held constant as described in Sec. II. We assume as in Sec. II that the wire-array mass m is changed by changing the diameter of each wire. We make the simplifying assumption that $F(r)$ (the normalized pinch current as a function of r, as defined in Sec. I) is held constant, so that $m/\tau_i^2 \propto I^2$, as indicated by Eqs. (1)–(3). We also assume that the total radiated x-ray energy $E_r \propto I^2$.

The peak radiated x-ray power P_r is proportional to E_r/τ_{th}:

$$P_r \propto \frac{E_r}{\tau_{th}} \propto \frac{I^2}{\tau_{th}}, \tag{18}$$

where τ_{th} is the thermalization time constant (i.e., the characteristic time over which the energy made available to the pinch is thermalized), as defined in Sec. III B. We approximate τ_{th} as

$$\tau_{th} \sim \frac{\delta}{v_f}, \tag{19}$$

where δ is an *effective* radial thickness of the imploding wire-array plasma, and v_f is an *effective* final pinch-implosion velocity. We assume δ is a power-law function of the ratio τ_a/τ_i,

$$\delta \propto \left(\frac{\tau_a}{\tau_i}\right)^{\zeta}, \tag{20}$$

where τ_a is the characteristic time required to ablate the wires, and ζ is a constant.

Analytic ablation calculations for a single frozen deuterium filament (not in an array) by Bobrova, Razinkova, and Sasorov [147] suggest that $\tau_a \propto m_s^{\gamma}[dI_s(t)/dt]^{-\eta}$, where m_s is the mass of a single filament, $I_s(t)$ is the current in the filament as a function of time, and $dI_s(t)/dt$, γ, and η are constants. According to the numerical results presented by Chittenden *et al.* in Fig. 1 of Ref. [39], $\eta \sim 1/2$ for a single aluminum wire not in an array. Assuming these scaling relations also apply to tungsten wires in an array, we have the following:

$$\tau_a \propto \frac{m_s^{\gamma}}{\left(\frac{dI_s(t)}{dt}\right)^{1/2}} = \frac{(m/n)^{\gamma}}{\left(\frac{dI(t)}{ndt}\right)^{1/2}}, \tag{21}$$

where m is the total-wire-array mass, $I(t)$ is the total-wire-array current as a function of time, and n is the number of wires in the array. Using Eqs. (19)–(21), we approximate the thermalization time τ_{th} as follows:

$$\tau_{th} \sim \frac{\delta}{v_f} \propto \left(\frac{\tau_a}{\tau_i}\right)^{\zeta} \tau_i \propto \frac{(m/n)^{\gamma\zeta}}{\left[\left(\frac{I}{n\tau_i}\right)^{\zeta/2} \tau_i^{\zeta}\right]} \tau_i, \tag{22}$$

where v_f is assumed to be proportional to τ_i^{-1}, and the characteristic value of $dI(t)/dt$ is estimated as I/τ_i, where I is the peak pinch current.

Coverdale *et al.* [148] have demonstrated that for aluminum-wire arrays, there exists a value of n that maximizes P_r—i.e., that P_r does not continue to increase indefinitely as n is increased. Mazarakis and co-workers [149–151] have shown that an optimum n also exists for the tungsten-wire-array system described in Sec. II. A polynomial fit [149–151] to the tungsten data suggests that P_r has a broad maximum at $n \sim 355$ and that P_r varies from 130 to 133 TW for $300 \leqslant n \leqslant 400$. Since P_r is proportional to E_r/τ_{th} [Eq. (18)], the expression for τ_{th} [Eq. (22)] must be indepen-

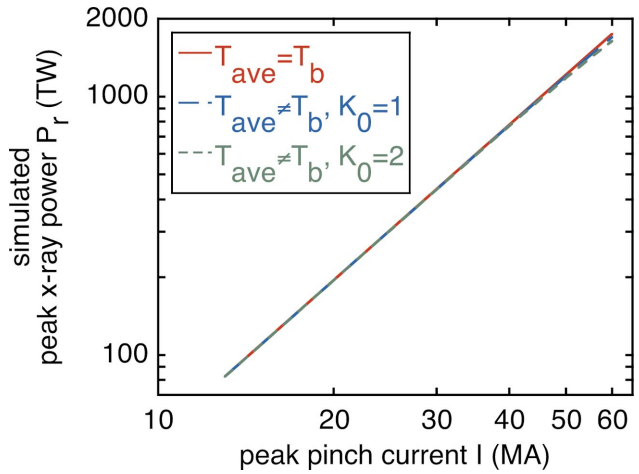

FIG. 10. (Color) Simulated peak radiated x-ray power P_r as a function of the peak pinch current I, for three cases. T_{ave} is the average pinch temperature, T_b is the pinch brightness temperature, and K_0 is an opacity multiplier.

dent of n for arrays that have a near-optimum number of wires. Hence for such arrays we have [according to Eq. (22)] that $\gamma=1/2$:

$$\tau_{th}\propto\left(\frac{m}{I\tau_i}\right)^{\zeta/2}\tau_i\,. \tag{23}$$

As discussed at the end of Sec. III B, the measured scaling of the peak x-ray power P_r with I suggests that for the experiments described in Secs. II and III A, $\tau_{th}\propto I^{1/2}\propto m^{1/4}$. Since for these experiments m was increased as I^2 and τ_i was held constant, we have from Eq. (23) that $\zeta=1$. Since we have assumed that $m/\tau_i^2\propto I^2$, we obtain from Eqs. (18)–(23) the following approximate expressions:

$$\delta\propto\frac{\tau_a}{\tau_i}\propto\left(\frac{m}{I\tau_i}\right)^{1/2}\propto m^{1/4}\propto(I\tau_i)^{1/2}, \tag{24}$$

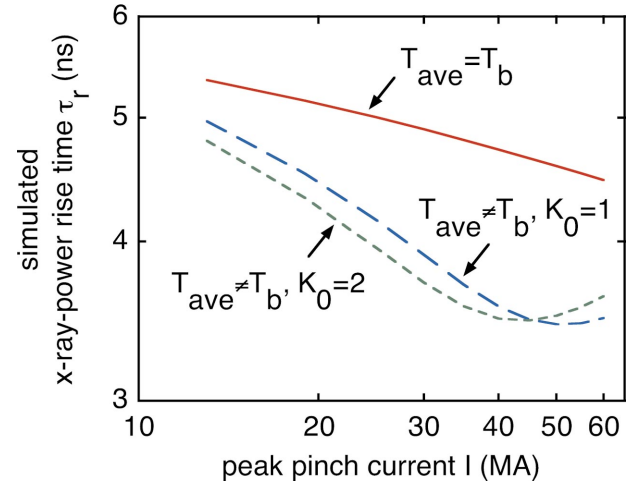

FIG. 11. (Color) Simulated 10%–90% x-ray-power rise time τ_r as a function of the peak pinch current I for three cases. T_{ave} is the average pinch temperature, T_b is the pinch brightness temperature, and K_0 is an opacity multiplier.

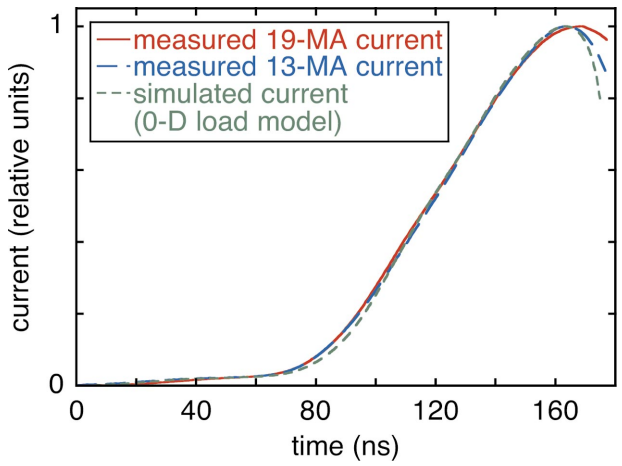

FIG. 12. (Color) Normalized pinch currents for the 13- and 19-MA peak-current shots. The 13-MA current trace is an average of the currents measured on shots 725 and 819; the 19-MA current is an average of the currents on shots 723, 724, 817, and 818. The normalized standard deviation of the pointwise difference between the two currents is less than 2%. Also plotted is the normalized simulated current, assuming the load can be modeled as an infinitely thin perfectly stable cylindrical foil.

$$\tau_{th}\sim\frac{\delta}{v_f}\propto\tau_a\propto\left(\frac{m\tau_i}{I}\right)^{1/2}\propto\frac{m^{3/4}}{I}\propto I^{1/2}\tau_i^{3/2}, \tag{25}$$

$$P_r\propto\frac{E_r}{\tau_{th}}\propto I^2\left(\frac{I}{m\tau_i}\right)^{1/2}\propto\frac{I^3}{m^{3/4}}\propto\left(\frac{I}{\tau_i}\right)^{3/2}. \tag{26}$$

As discussed above, Eqs. (24)–(26) assume that the wire-mass density, number of wires, wire-array diameter, wire-array length, and normalized pinch-current $F(r)$ are held constant, and that the number of wires is near the value that optimizes P_r. Equation (26) also makes the simplifiying assumption that $E_r\propto I^2$. Since Eqs. (24)–(26) assume that δ is determined by τ_a (and hence m), we expect these expres-

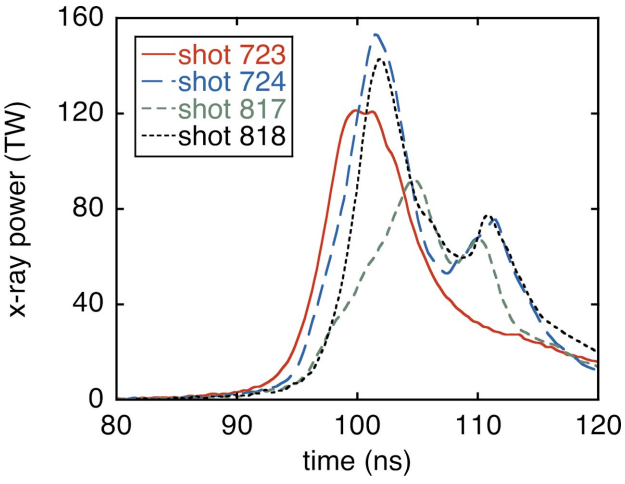

FIG. 13. (Color) X-ray power as a function of time for four nominally identical shots. The time is from the extrapolated beginning of the load current; hence, the plots directly show shot-to-shot fluctuations in the implosion time.

sions to become inaccurate when m (or more generally, the mass per unit length m/ℓ) is sufficiently small—i.e., when wire ablation no longer determines δ.

Each of Eqs. (24)–(26) leads to an interesting observation. According to Eq. (24), if m is increased as I^2 to keep τ_i constant (as we did for the experiments described in Secs. II and III A), then $\tau_a \propto m^{1/4} \propto I^{1/2}$: i.e., τ_a increases as $I^{1/2}$ while τ_i remains fixed. At sufficiently high current, such scaling leads to an ablation time that is longer than the implosion time, which may not be the optimum manner in which to increase I in future accelerators.

According to Eq. (25), to keep τ_{th} constant as I is increased, τ_i would have to be scaled as follows:

$$\tau_i \propto I^{-1/3}, \tag{27}$$

which is equivalent to increasing m as $I^{4/3}$. If Eq. (25) is valid, Eq. (27) might be one approach to achieve I^2 x-ray-power scaling. Such an approach would, in addition, increase the implosion velocity v_f as $I^{1/3}$, which would increase the thermalization efficiency of the pinch's kinetic energy.

According to Eq. (26), P_r can be made to scale as I to a power higher than 2. For example, when

$$\tau_i \propto I^{-1}, \tag{28}$$

which requires holding m constant as I is increased, then τ_{th} is proportional to I^{-1} and P_r increases approximately as I^3. Decreasing τ_i as I is increased [according to either Eq. (27) or (28)] would, however, increase significantly the size and cost of future accelerators, since to zeroth order accelerator voltages near the pinch scale as I/τ_i. In addition, we note that if I^3 power scaling could be demonstrated for $I > 13$ MA, the 1200-TW x-ray-power requirement for high-yield ICF would be met at 32 MA, but a higher current would still be necessary to meet the ~8-MJ x-ray-energy requirement.

Equations (24)–(26) appear to be consistent with the pinch-current measurements presented in Fig. 12. In this figure, we plot the normalized pinch currents measured for both the 13- and 19-MA peak-current shots. We also plot the normalized calculated current assuming that the wire array can be modeled as an infinitely thin perfectly stable cylindrical foil [Eqs. (1)–(3)]. The normalized calculated current is obtained from a circuit simulation and is essentially identical at both 13 and 19 MA when the pinch mass m in the simulations is scaled as I^2.

The standard deviation of the pointwise difference between the normalized current measurements at 13 and 19 MA (plotted in Fig. 12) is less than 2%. Until peak current, all three normalized wave forms are similar. After peak current, however, the 19-MA measurement is significantly less like the simulation than that at 13 MA. If the measured currents are accurate after their peaks, this difference would imply that, late in the implosion, the pinch inductance is greater at 13 than at 19 MA. This would be consistent with the mass ablating and assembling on axis over a longer period of time at the higher current, producing a more diffuse pinch and a softer (less-well-defined) implosion [17,68].

We caution, however, that as indicated in Fig. 2, the pinch-current monitors were located 6 cm from the axis of the pinch—i.e., in a severe environment. The voltage near the location of these monitors increased rapidly after peak current and, in addition, was ~50% higher at 19 MA than at 13 MA. Because of the corresponding increased electron deposition in the anode hardware near the pinch [120,122,127,140–143], the current measurements are less accurate after peak at 19 than at 13 MA. As discussed in Sec. II, we estimate that at 19 MA, the error (due to electron damage) at peak current is 2%.

3. Suggestions for future work

Equations (24)–(26) suggest that for the wire array described in Sec. II, quadratic x-ray-power scaling will be achieved if τ_i is scaled as $I^{-1/3}$. Quadratic scaling might also be demonstrated with the use of an alternate wire material [146,152], an optimized nested wire array [146], a foil [152], or an optimized current pre-pulse [57,68,153]. Because wire ablation evolves in the r-θ plane and the Rayleigh-Taylor instability develops in r-z, *predictive* three-dimensional radiative-MHD simulations of the ablation, implosion, and stagnation of an array may ultimately be required to design an optimized pinch-accelerator system. The experimental configuration (Fig. 2) was kept relatively uncomplicated to facilitate use of the measurements at 13 and 19 MA to validate such simulations. (We note that present two-dimensional pinch simulations are *not* predictive, since they assume an arbitrary amplitude for the seed of the Rayleigh-Taylor instability. The peak x-ray power and power rise time are strong functions of the initial seed. In the present simulations, the seed amplitude is arbitrarily adjusted until results match experiment. At this time, there is no *a priori* method for determining what the seed amplitude should be or how it scales with I.)

IV. SHOT-TO-SHOT FLUCTUATIONS

A. Measurements

Measurements of the 1σ shot-to-shot fluctuations in P_r, E_r, τ_r, τ_w, and τ_i as functions of I are summarized in Table II. We define the implosion time τ_i to be the time interval between the extrapolated beginning of the load current and the extrapolated beginning of the x-ray-power pulse. Shot-to-shot variations in the temporal and spatial structure of the x-ray emission are presented in Figs. 13–15.

The 1σ fluctuations in P_r listed in Table II are determined as follows. (The fluctuations in E_r, τ_r, τ_w, and τ_i are obtained in a similar manner.) As discussed in Sec. III A, it appears that gap closure did not affect P_r on shots 566, 594, 597, 647–649, 683, 723-725, and 817–820. We assume (as in Sec III A) that the data for these 14 shots can be fit to a power-law function of I and use the least-squares method to estimate that $P_r = \beta_1 I^{1.2428}$, where $\beta_1 = 1.187 \times 10^5$ (in SI units). This power-law scaling is discussed in Sec. III A and is plotted in Fig. 7. (For the calculations in this section and the results listed in Table II, we use more precise values for

TABLE II. Summary of the measured shot-to-shot fluctuations. The fluctuations are those observed for one-half of the pinch and have been corrected for the fluctuations inherent in the diagnostic systems. Assuming that the half observed radiates in a manner that is statistically independent of the other half, the fluctuations for the entire pinch are a factor of $2^{1/2}$ less than those listed here. (In SI units, $\beta_1=1.187\times10^5$, $\beta_2=3.873\times10^{-7}$, $\beta_3=2.017\times10^{-6}$, $\beta_4=7.508\times10^{-12}$, $\beta_5=6.162\times10^{-12}$, and $\beta_6=7.395\times10^2$.)

	1σ fluctuation, assuming it is independent of the peak pinch current	Z shot numbers	1σ fluctuation at 13 MA	13-MA Z shot numbers	1σ fluctuation at 19 MA	19-MA Z shot numbers	1σ random fluctuation in the response of the diagnostic system
Peak radiated x-ray power P_r ($P_r=\beta_1 I^{1.2428}$)	$(12\pm2.5)\%$	566, 594, 597, 647–649, 683, 723–725, 817–820	$(12\pm4.1)\%$	647–649, 725, 819, 820	$(14\pm4.1)\%$	566, 594, 597, 683, 723, 724, 817, 818	2.3%
Total radiated x-ray energy E_r (bolometers) ($E_r=\beta_2 I^{1.7342}$)	$(9.1\pm2.6)\%$	647, 649, 723–725, 817–819	$(8.7\pm4.4)\%$	647, 649, 725, 819	$(13\pm6.7)\%$	723, 724, 817, 818	1.8%
Total radiated x-ray energy E_r (calorimeter) ($E_r=\beta_3 I^{1.6451}$)	$(7.4\pm2.1)\%$	647, 649, 723–725, 817–819	$(7.9\pm4.0)\%$	647, 649, 725, 819	$(11\pm5.6)\%$	723, 724, 817, 818	4.5%
X-ray-power rise time τ_r ($\tau_r=\beta_4 I^{0.3883}$)	$(26\pm5.3)\%$	566, 594, 597, 647–649, 683, 723–725, 817–820	$(27\pm9.6)\%$	647–649, 725, 819, 820	$(29\pm8.5)\%$	566, 594, 597, 683, 723, 724, 817, 818	2.9%
X-ray-power pulse width τ_w ($\tau_w=\beta_5 I^{0.4544}$)	$(8.7\pm2.5)\%$	647, 649, 723–725, 817–819	$(10\pm5.1)\%$	647, 649, 725, 819	$(11\pm5.6)\%$	723, 724, 817, 818	2.3%
Pinch-implosion time τ_i ($\tau_i=\beta_6 m^{1/2}/I$)	$(2.4\pm0.5)\%$	566, 594, 597, 647–649, 683, 723–725, 817–820	$(1.1\pm0.4)\%$	647–649, 725, 819, 820	$(3.3\pm0.9)\%$	566, 594, 597, 683, 723, 724, 817, 818	0.5%

the power-law exponents than were given in Sec. III.)

To quantify the fluctuations in P_r, we assume the following statistical model. We express the jth measurement of P_r as

$$P_{rj}=\beta_1 I_j^{1.2428}+\varepsilon_j, \tag{29}$$

where ε_j is the random fluctuation in P_{rj}, and I_j is the jth measurement of the peak pinch current I. Assuming Eq. (29) and using all 14 data points in Fig. 7, we estimate the sample fractional standard deviation σ of the measurements of P_r as follows:

$$\sigma=\left[\frac{1}{14-2}\sum_{j=1}^{14}\left(\frac{P_{rj}-\beta_1 I_j^{1.2428}}{\beta_1 I_j^{1.2428}}\right)^2\right]^{1/2}. \tag{30}$$

(We subtract 2 from 14 since two degrees of freedom were used to obtain the power-law curve.) We find that σ, which we also refer to as the 1σ shot-to-shot fluctuation, is 12.3%. The estimated 1σ variation due to the detector system is 2.3%; subtracting this in quadrature gives 12.1% for the corrected value for σ. (We include only two significant figures in Table II.) We estimate the uncertainty in σ to be $\sigma/[2(14-2)]^{1/2}=2.5\%$ [154,155].

The 1σ fluctuations in E_r, τ_r, τ_w, and τ_i are estimated using expressions similar to Eqs. (29) and (30). To estimate the 1σ fluctuation in τ_i, we assume as indicated in Table II that without fluctuations,

$$\tau_i\propto m^{1/2}/I. \tag{31}$$

Equation (30) and similar equations for E_r, τ_r, τ_w, and τ_i assume that the fluctuations are independent of I. Treating the 13-MA shots separately from the shots at 19 MA, we find (as indicated in Table II) that within statistical uncertainties, the fluctuations in P_r, E_r, τ_r, and τ_w are the same at both 13 and 19 MA—although there appears to be a trend with increasing I. Additional measurements would be needed to improve the precision of these results.

The 1σ fluctuations presented in Table II are for the half of the pinch viewed by the x-ray diagnostics. If the half

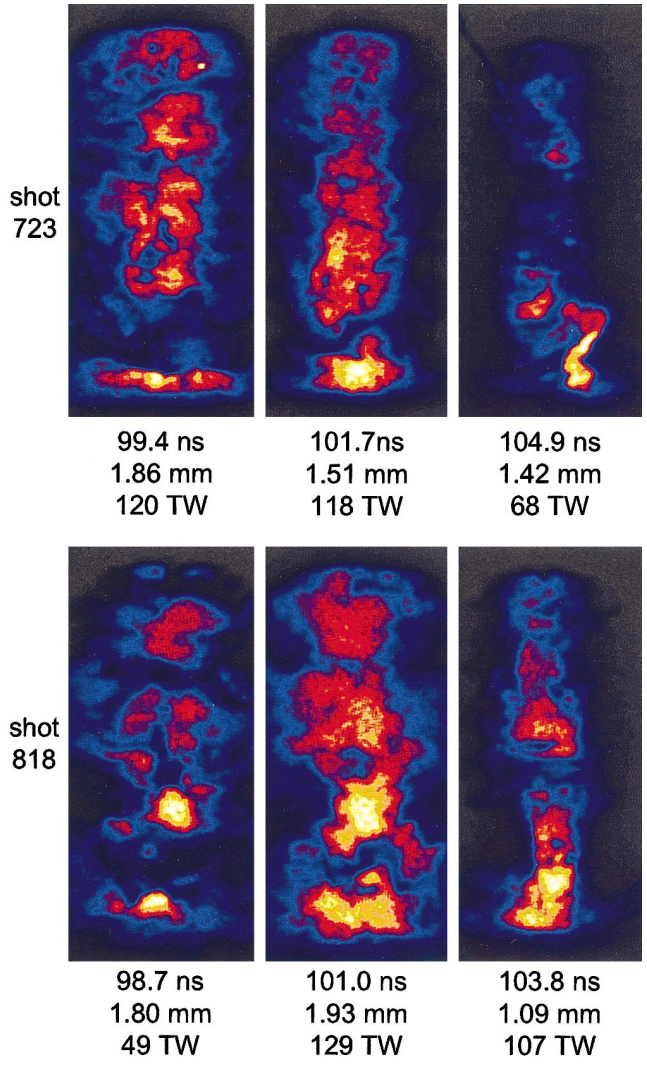

FIG. 14. (Color) Time-resolved x-ray images for two nominally identical shots. The time is from the extrapolated beginning of the load current. Each image represents a 3.9 mm×8.5 mm field of view. The distance listed beneath each figure is the full width at half maximum of the pinch obtained by integrating the image in the axial direction.

observed radiates in a manner that is statistically independent of the other half, the fluctuations for the entire pinch would be smaller by a factor of $2^{1/2}$ than the values presented in this table. (A more complete discussion of this point is given in the Appendix.)

We note that the 1σ fluctuations in P_r and E_r listed in Table II are consistent, within experimental error, with recent measurements by Cuneo [146] using a similar pinch configuration. However, the fluctuations that were obtained [146] for one-half of the pinch in τ_r and τ_i are $(8.8\pm3)\%$ and $(0.8\pm0.3)\%$, respectively, which are significantly less than the values reported here. The source of these discrepancies is not yet understood. Our results appear consistent with the 15% shot-to-shot fluctuations in the peak radiated aluminum-K-shell power reported by Sanford and co-workers [61] for various aluminum wire arrays. (The fraction of the pinch viewed in these experiments was 70%.). The 1σ fluctuations

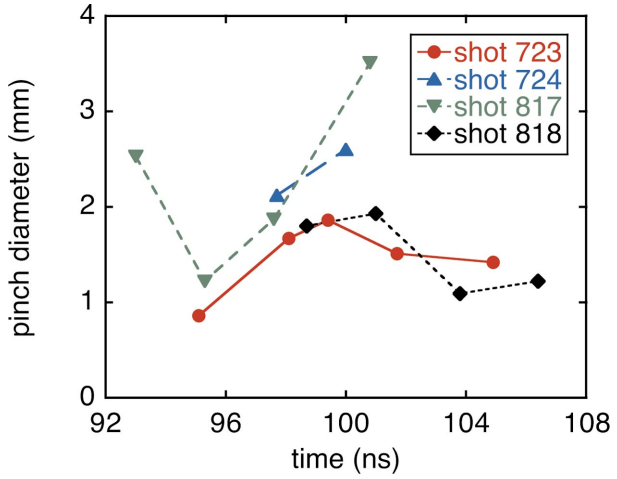

FIG. 15. (Color) The axially integrated full width at half maximum of the x-ray emission from the pinch, as a function of time, for four nominally identical shots. The measurements were obtained from images such as those shown in Fig. 14. The time is from the extrapolated beginning of the load current. The symbols indicate the measurements; the lines are included to aid the eye.

in P_r and τ_w reported by Sanford *et al.* in Ref. [114] for a tungsten wire array imploding upon a centrally located foam target are (for one half of the pinch) $(22\pm5)\%$ and $(25\pm6)\%$, respectively, which are within a factor of 2–3 of the values listed in Table II.

Temporally and spatially resolved x-ray measurements obtained on shots with nominally identical geometries and pinch currents are presented in Figs. 13–15. Figure 13 plots the peak x-ray power as a function of time for four shots (723, 724, 817, and 818), and shows significant shot-to-shot fluctuations in the x-ray-power time history. For each of these four plots, the time is referenced to the extrapolated beginning of the pinch current; hence the plots

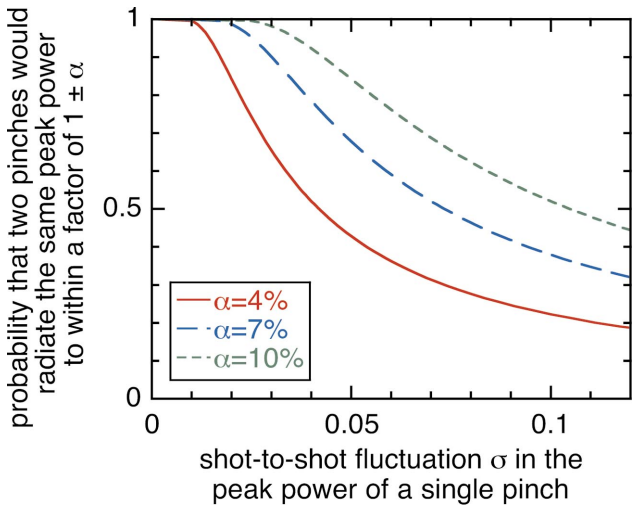

FIG. 16. (Color) The approximate probability that on a given shot, two independent pinches (in a double-pinch ICF driver) would radiate the same peak x-ray power to within a factor of $1\pm\alpha$ (where $0\leqslant\alpha\ll1$) as a function of σ (the fractional 1σ shot-to-shot fluctuation in the peak power radiated by a single pinch). Curves are plotted for three different values of α.

directly display shot-to-shot fluctuations in the implosion time. For two of these shots, Fig. 14 presents images of the pinch obtained with the x-ray camera, which exhibit significant shot-to-shot variations in the spatial structure of the x-ray emission. Such images were used to determine the axially integrated pinch diameter as a function of time presented in Figs. 14 and 15. Figures 13–15 illustrate that significant, apparently random shot-to-shot fluctuations are possible in the implosion and radiation histories of nominally identical shots.

B. Calculation of the shot-success probability of the *z*-pinch-driven hohlraum

Random fluctuations in the x-ray emission of the two pinches in the double-pinch ICF driver [44,48,87,88,110–112,118] would affect the symmetry of the radiation driving the capsule implosion. In this section, we estimate the effect of such variations on the probability that a shot taken with this configuration would be successful. We begin by calculating the probability that on a given shot, the two pinches would have the same peak x-ray power P_r to within a factor of $1\pm\alpha$, where $0\leqslant\alpha\ll 1$. We assume first that the x-ray powers emitted by the two pinches would have identical normalized time histories, with peaks that occur at exactly the same time. Hence we assume that only the amplitudes of the two x-ray-power pulses would differ. The effect of differences in the normalized time histories is briefly discussed at the end of this section.

We assume that the peak power P_r of a single pinch would have a normal probability distribution [156] with mean value μ and fractional standard deviation (1σ variation) σ. We assume that the two pinches in the double-pinch system would be independent of each other and have identical P_r probability distributions. Let x denote the peak radiated power of the first pinch and y the power of the second on any given shot. Then the probability $dp(x)dp(y)$ that the power of the first would lie between x and dx and the power of the second between y and dy is given by [156]

$$dp(x)dp(y)=\frac{1}{\sigma\mu\sqrt{2\pi}}\exp\left(\frac{-(x-\mu)^2}{2\sigma^2\mu^2}\right)dx \times\frac{1}{\sigma\mu\sqrt{2\pi}}\exp\left(\frac{-(y-\mu)^2}{2\sigma^2\mu^2}\right)dy. \quad (32)$$

[Equation (32) differs from the expression given in [156] because here we define σ to be the *fractional* standard deviation.] The probability p that the power of the second pinch y would lie within a factor of $1\pm\alpha$ of x is given by

$$p=\frac{1}{2\pi\sigma^2\mu^2}\int_{-\infty}^{+\infty}\exp\left(\frac{(x-\mu)^2}{2\sigma^2\mu^2}\right)dx \times\int_{x(1-\alpha)}^{x(1+\alpha)}\exp\left(\frac{(y-\mu)^2}{2\sigma^2\mu^2}\right)dy. \quad (33)$$

The quantity p is the probability that the two pinches in the z-pinch-driven hohlraum would radiate the same peak power to within a factor of $1\pm\alpha$.

For a typical experiment to be successful, the x-ray powers x and y must not only be similar to each other, but also within a few standard deviations of the mean μ. Strictly speaking, the above integral should be carried out only over x-ray powers of interest (i.e., near the peak value μ), but since the integrand is negligible outside this region, the above is a reasonable approximation.

Defining $s\equiv(x-\mu)/\sigma\mu$ and $u\equiv(y-\mu)/\sigma\mu$, we can simplify Eq. (33) as

$$p=\frac{1}{2\pi}\int_{-\infty}^{+\infty}\exp\left(\frac{-s^2}{2}\right)ds\int_{s-\alpha s-(\alpha/\sigma)}^{s+\alpha s+(\alpha/\sigma)}\exp\left(\frac{-u^2}{2}\right)du. \quad (34)$$

If $1/\sigma\gg 1$, then the integrand is significant only when $s\ll 1/\sigma$. Hence Eq. (34) can be approximated as

$$p=\frac{1}{2\pi}\int_{-\infty}^{+\infty}\exp\left(\frac{-s^2}{2}\right)ds\int_{s-(\alpha/\sigma)}^{s+(\alpha/\sigma)}\exp\left(\frac{-u^2}{2}\right)du. \quad (35)$$

This expression can be evaluated in a coordinate system rotated 45° counterclockwise from the (s,u) system. This transformation $[w\equiv(u+s)/2^{1/2}, z\equiv(u-s)/2^{1/2}]$ allows us to write Eq. (35) as

$$p=\frac{1}{2\pi}\int_{-\infty}^{+\infty}\exp\left(\frac{-w^2}{2}\right)dw\int_{-\alpha/\sigma\sqrt{2}}^{\alpha/\sigma\sqrt{2}}\exp\left(\frac{-z^2}{2}\right)dz =\mathrm{erf}\left(\frac{\alpha}{2\sigma}\right). \quad (36)$$

Hence the probability p that x and y are within a factor $1\pm\alpha$ of each other is approximately equal to $\mathrm{erf}(\alpha/2\sigma)$.

Figure 16 plots p as a function of σ, with α as a parameter. To achieve a 90% probability of success would require that $\alpha/2\sigma=1.16$ [156]. Thus, if the peak x-ray powers of the two pinches in a future ICF driver are to be within 7% of each other ($\alpha\leqslant 7\%$) on at least 90% of the shots, then the 1σ fluctuation in the power radiated by a single pinch σ must be less than or equal to 3%.

Presently, as indicated in Table II, $\sigma\sim 12\%$ for one-half of the pinch, assuming σ is independent of I. As discussed in the Appendix, we estimate that for the entire pinch $\sigma\sim(12/2^{1/2})\%=8.5\%$. When $\alpha=7\%$ and $\sigma=8.5\%$, the success probability p is 44% [156]. Consequently, to develop a z-pinch-driven hohlraum with a 90% shot-success probability, it will be necessary either to reduce the random fluctuations in P_r below present levels, to decrease the sensitivity of the capsule and hohlraum designs to a power imbalance, or to make progress in both areas. We note, however, that a 44% success rate may be acceptable for experiments conducted on a prototype thermonuclear-fusion driver.

The calculation above gives the probability that on a given shot, the two pinches would radiate the same peak power P_r to within the factor $1\pm\alpha$. The symmetry of the

radiation-drive history in a double-pinch system would, however, also be a function of differences in the normalized time histories of the two x-ray-power pulses—i.e., differences in E_r, τ_r, τ_i, etc. We estimate that the probability P that a double-pinch shot would simultaneously meet all of the requirements to drive a capsule symmetrically is given by

$$P \equiv \prod_i p_i \equiv \prod_i \mathrm{erf}\left(\frac{\alpha_i}{2\sigma_i}\right), \tag{37}$$

where the product is over all of the relevant factors, assuming that the p_i's are statistically independent of each other. The symmetry requirements (α_i's) for the relevant variables (such as E_r, τ_r, τ_i, etc.) are presently being developed. When these have been determined, Eq. (37) can be used to estimate the shot-success probability P as a function of the α_i's and σ_i's.

C. Discussion

1. MHD simulations

The observed shot-to-shot fluctuations described in Sec. IV A are consistent, to within a factor of 4, with two-dimensional MHD simulations performed by Hammer *et al.* [44]. These simulations assume lithium deuteride instead of tungsten for the pinch material and a peak pinch current of $\sim$63 MA. Random-mass-density perturbations were introduced to initiate growth of the Rayleigh-Taylor instability. As indicated in Table I of Ref. [44], the simulations show that with a 1% perturbation amplitude, changing only the random number *seed* (while holding the *amplitude* of the perturbation level constant at 1%) can change both the peak radiated x-ray power and the x-ray-power pulse width by 30%. MHD simulations performed by Peterson *et al.* [157] for an aluminum-foil pinch with a 3.4-MA peak current and a 1.9-μs implosion time demonstrate that changing the *pattern* of the random-mass-density perturbations while keeping the *amplitude* constant can have a significant effect on the mass-density distribution at stagnation (Fig. 7 of [157].) These results [44,157] are in qualitative agreement with the measurements presented in Table II and Figs. 13–15.

2. Suggestions for future work

The calculations described in Refs. [44] and [157] demonstrate that the evolution of a pinch is a sensitive function of initial conditions. This sensitivity, the simulated mass-density profiles of an imploding pinch presented in [44,157,158], and Figs. 13–15 are suggestive of spatiotemporal chaos [159–162]. We propose that additional MHD simulations be performed to determine whether the evolution of a z pinch is, in fact, chaotic.

Specifically, we propose that simulations quantify more completely the sensitivity of the evolution and radiation emission of a pinch to the random number used to seed the Rayleigh-Taylor instability, and to small changes in the mass, wire-array diameter, peak current, and other pinch parameters. It would be interesting to determine the sensitivity for various pinch materials and to quantify how the sensitivity changes as the peak current is increased above 19 MA. The ultimate goal, of course, would be to develop for ICF applications a new pinch configuration that is less sensitive to initial conditions. Because the ablation of the wire mass evolves in the r-θ plane and the Rayleigh-Taylor instability develops in r-z, three-dimensional radiative-MHD simulations may ultimately be required for such numerical studies to be meaningful. We also propose that kinetic effects be considered as possible contributors to the shot-to-shot fluctuations.

ACKNOWLEDGMENTS

The authors are deeply indebted to L. Longmire, S. Glaros, M. Johnson, P. Reynolds, R. Green, J. Trammell, and R. Flora for invaluable contributions, and to T. Pointon, T. Cutler, and E. Waisman for graciously reviewing this article. We also wish to thank our colleagues at Sandia National Laboratories, Ktech Corporation, Team Specialty Products, Tri-Tech Machine Tool Company, Gull Group, Bechtel, C-Lec Plastics, Cornell University, EG&G, Imperial College, Lawrence Livermore National Laboratory, Los Alamos National Laboratories, Mission Research Corporation, Naval Research Laboratory, Prodyn Technologies, Titan-Pulse Sciences Division, the University of California, the University of Nevada, the University of New Mexico, Votaw Precision Technologies, and the Weizmann Institute for critical discussions. Sandia is a multiprogram laboratory operated by Sandia Corporation, a Lockheed Martin Company, for the U.S. Department of Energy under Contract No. DE-AC04-94-AL85000.

APPENDIX

The results presented in Table II are based on the radiation emitted from one-half of the pinch. Thus it is appropriate to examine how we might infer from these measurements the 1σ fluctuations for the entire pinch. The discussion below is given in terms of P_r; similar discussions can be developed for E_r, τ_r, τ_w, and τ_i.

We idealize the pinch as one dimensional with length ℓ. We envision the x-ray emission occurring from L segments, each with equal length ℓ/L. Let ξ_i denote the x-ray power emitted from the ith segment when the total x-ray power is at its peak value. The total power Ξ_L radiated by the pinch is then given by

$$\Xi_L = \sum_{i=1}^{L} \xi_i . \tag{A1}$$

As a result of an aperture near the pinch, the diagnostics that view the pinch do not view all L segments but rather a contiguous set of $K<L$, constituting a length $K\ell/L=k$ and yielding a peak power Ξ_K:

$$\Xi_K = \sum_{i=j}^{K+j-1} \xi_i . \tag{A2}$$

We denote the ratio $k/\ell = K/L$ as the view factor, which is 1/2 for the experiments described above.

Any estimation of the fluctuations in Ξ_L from observations of Ξ_K depends on a statistical model, which makes assumptions about the emission from each segment and relationships between segments. We consider three such hypothetical models and estimate in each case σ_L, the fractional standard deviation in Ξ_L, from σ_K, the observed fractional standard deviation in Ξ_K.

Model 1. Statistically independent emission. We assume first that each x-ray-emitting segment of the pinch is independent of the others, and that the ξ_i's all have the sample normal probability distribution with the same mean and standard deviation. It is then easy to show that the mean values $\langle \Xi_L \rangle$ and $\langle \Xi_K \rangle$ of Ξ_L and Ξ_K, respectively, are related as $\langle \Xi_L \rangle = (\ell/k)\langle \Xi_K \rangle$. The fractional standard deviations are related as $\sigma_L = (k/\ell)^{1/2}\sigma_K$. According to this model, if the x-ray diagnostics view one-half of the pinch ($k/\ell = 1/2$) and if the measurements of the average peak power and its fractional standard deviation for the half observed are 65 TW and 12%, respectively, then one would infer 130 TW for the average peak power from the whole pinch, with an associated fractional standard deviation of 8.5%.

Model 2. Statistically coupled emission. For this model we assume that the emission ξ_i from each segment can be expressed as $\xi_i = h\Lambda$, where h is a constant that *does not* fluctuate from shot to shot and Λ is a random variable that *does* fluctuate from shot to shot. Thus, each segment of the pinch fluctuates in brightness from shot to shot, but fluctuations from different segments are in phase. As in model 1, the mean values $\langle \Xi_L \rangle$ and $\langle \Xi_K \rangle$ are related by $\langle \Xi_L \rangle = (\ell/k)\langle \Xi_K \rangle$. However, since the fluctuations in emission from each segment derive from the single random variable Λ, the fractional standard deviations are equal: $\sigma_L = \sigma_K$. If a *z* pinch behaved in this manner, one would infer that the relative shot-to-shot fluctuations in the peak power radiated by the entire pinch would be the same as in any measured portion of the pinch.

Model 3. Emission constrained by a conservation law. One might speculate that most segments in a *z* pinch radiate randomly and almost independently but that some physical constraint (e.g., the total current transferred or total electrical power) fixes the peak radiated x-ray power from the whole pinch. In this case, Ξ_L is fixed and $\sigma_L = 0$. Yet depending on K, the measured quantity Ξ_K may fluctuate from shot to shot, which makes $\sigma_K \neq 0$.

At best, each of these simple models only partially characterizes the *z*-pinch plasma. Model 1 assumes there is no correlation between x-ray-emitting hot spots in the pinch. This cannot be entirely true, since physical variables (e.g., the magnetic field) exist that connect points within the plasma. Moreover, as each hot spot radiates, energy is removed from the plasma system. By contrast, model 2 assumes that all of the emitting points are statistically coupled, suggesting that shot-to-shot variations in the x-ray emission are dominated by effects other than the pinch process itself. For example, there may be some parasitic electrical current path [17] that bypasses the pinch and that varies from shot to shot. However, framing-camera pictures indicate different arrangements of hot spots as a function of time and from shot to shot, suggesting that more than one variable is at work in causing peak-power fluctuations. Model 3 assumes that some over riding conservation law limits the peak power emitted from the whole pinch. This may represent an efficiency constraint: that is, while the locations and brightness of hot spots may vary from shot to shot, only a certain amount of total power can be radiated for a fixed input. Estimates of the peak radiated power from the whole pinch, but derived from measurements of a fraction of the pinch, could fluctuate because of the changing locations of the hot spots. In addition, apertured measurements would not suggest the existence of a conservation law.

We make the tentative assumption that model 1 is most correct with respect to peak-x-ray-power emission—in particular, that shot-to-shot fluctuations for the entire pinch are a factor of $2^{1/2}$ less than fluctuations measured by diagnostics viewing only 1/2 of the pinch. This is consistent with preliminary experiments performed with the slotted electrode shown in Fig. 2 replaced by a nearly solid enclosure to form a hohlraum. For such a configuration, measurements of the hohlraum-wall temperature in effect integrate over the radiation emitted from the entire pinch. Such measurements on eight Z-accelerator shots [146] suggest that the 1σ variation in the peak radiated power from the entire pinch is $(7.3 \pm 2.1)\%$, which is reasonably consistent with the value $(12 \pm 2.5)\%/2^{1/2} = (8.5 \pm 1.8)\%$ inferred from the results presented in Sec. IV A. These, however, are preliminary observations, and additional experiments are needed to determine more precisely how the fluctuations from an entire pinch can be inferred from measurements made on a fraction of the pinch length.

[1] P. J. Turchi and W. L. Baker, J. Appl. Phys. **44**, 4936 (1973).
[2] D. Mosher, S. J. Stephanakis, I. M. Vitkovitsky, C. M. Dozier, L. S. Levine, and D. J. Nagel, Appl. Phys. Lett. **23**, 429 (1973).
[3] C. Stallings, K. Nielsen, and R. Schneider, Appl. Phys. Lett. **29**, 404 (1976).
[4] H. W. Bloomberg, M. Lampe, and D. G. Colombant, J. Appl. Phys. **51**, 5277 (1980).
[5] F. S. Felber and N. Rostoker, Phys. Fluids **24**, 1049 (1981).
[6] W. Clark, M. Wilkinson, J. Rauch, and J. LePage, J. Appl. Phys. **53**, 1426 (1982).
[7] W. Clark, M. Gersten, J. Katzenstein, J. Rauch, R. Richardson, and M. Wilkinson, J. Appl. Phys. **53**, 4099 (1982).
[8] S. M. Zakharov, G. V. Ivanenkov, A. A. Kolomenskii, S. A. Pikuz, and A. I. Samokhin, Sov. J. Plasma Phys. **13**, 115 (1987).

[9] I. K. Aivazov, V. D. Vikharev, G. S. Volkov, L. B. Nikandrov, V. P. Smirnov, and V. Ya. Tsarfin, Sov. J. Plasma Phys. **14**, 110 (1988).
[10] M. V. Bekhtev, V. D. Vikharev, S. V. Zakharov, V. P. Smirnov, M. V. Tulupov, and V. Ya. Tsarfin, Sov. Phys. JETP **68**, 955 (1989).
[11] V. P. Smirnov, Plasma Phys. Controlled Fusion **33**, 1697 (1991).
[12] D. H. Kalantar and D. A. Hammer, Phys. Rev. Lett. **71**, 3806 (1993).
[13] J. W. Thornhill, K. G. Whitney, C. Deeney, and P. D. LePell, Phys. Plasmas **1**, 321 (1994).
[14] E. J. Yadlowsky, T. B. Settersten, R. C. Hazelton, J. J. Moschella, G. G. Spanjers, J. P. Apruzese, and J. Davis, Rev. Sci. Instrum. **66**, 652 (1995).
[15] S. Maxon, J. H. Hammer, J. L. Eddleman, M. Tabak, G. B. Zimmerman, W. E. Alley, K. G. Estabrook, J. A. Harte, T. J. Nash, T. W. L. Sanford, and J. S. De Groot, Phys. Plasmas **3**, 1737 (1996).
[16] T. W. L. Sanford, G. O. Allshouse, B. M. Marder, T. J. Nash, R. C. Mock, R. B. Spielman, J. F. Seamen, J. S. McGurn, D. Jobe, T. L. Gilliland, M. Vargas, K. W. Struve, W. A. Stygar, M. R. Douglas, M. K. Matzen, J. H. Hammer, J. S. De Groot, J. L. Eddleman, D. L. Peterson, D. Mosher, K. G. Whitney, J. W. Thornhill, P. E. Pulsifer, J. P. Apruzese, and Y. Maron, Phys. Rev. Lett. **77**, 5063 (1996).
[17] E. J. Yadlowsky, J. J. Moschella, R. C. Hazelton, T. B. Settersten, G. G. Spanjers, C. Deeney, B. H. Failor, P. D. LePell, J. Davis, J. P. Apruzese, K. G. Whitney, and J. W. Thornhill, Phys. Plasmas **3**, 1745 (1996), and references therein.
[18] J. Davis, N. A. Gondarenko, and A. L. Velikovich, Appl. Phys. Lett. **70**, 170 (1997).
[19] C. Deeney, J. McGurn, D. Noack, J. L. Porter, R. B. Spielman, J. F. Seamen, D. O. Jobe, M. F. Vargas, T. Gilliland, M. R. Douglas, and M. K. Matzen, Rev. Sci. Instrum. **68**, 653 (1997).
[20] C. Deeney, T. J. Nash, R. B. Spielman, J. F. Seamen, G. C. Chandler, K. W. Struve, J. L. Porter, W. A. Stygar, J. S. McGurn, D. O. Jobe, T. L. Gilliland, J. A. Torres, M. F. Vargas, L. E. Ruggles, S. Breeze, R. C. Mock, M. R. Douglas, D. L. Fehl, D. H. McDaniel, M. K. Matzen, D. L. Peterson, W. Matuska, N. F. Roderick, and J. J. MacFarlane, Phys. Rev. E **56**, 5945 (1997).
[21] J. S. De Groot, A. Toor, S. M. Golberg, and M. A. Liberman, Phys. Plasmas **4**, 737 (1997).
[22] M. K. Matzen, Phys. Plasmas **4**, 1519 (1997).
[23] R. E. Olson, J. L. Porter, G. A. Chandler, D. L. Fehl, D. O. Jobe, R. J. Leeper, M. K. Matzen, J. S. McGurn, D. D. Noack, L. E. Ruggles, P. Sawyer, J. A. Torres, M. Vargas, D. M. Zagar, H. N. Kornblum, T. J. Orzechowski, D. W. Phillion, L. J. Suter, A. R. Thiessen, and R. J. Wallace, Phys. Plasmas **4**, 1818 (1997).
[24] J. L. Porter, Bull. Am. Phys. Soc. **42**, 1948 (1997).
[25] J. H. Brownell, R. L. Bowers, K. D. McLenithan, and D. L. Peterson, Phys. Plasmas **5**, 2071 (1998).
[26] C. Deeney, M. R. Douglas, R. B. Spielman, T. J. Nash, D. L. Peterson, P. L'Eplattenier, G. A. Chandler, J. F. Seamen, and K. W. Struve, Phys. Rev. Lett. **81**, 4883 (1998). (A peak x-ray power of 280 TW is quoted in this reference for the optimized wire-array configuration. More recent measurements suggest the power is ~230 TW.)
[27] C. Deeney, D. L. Peterson, R. B. Spielman, K. W. Struve, and G. A. Chandler, Phys. Plasmas **5**, 2605 (1998).
[28] M. R. Douglas, C. Deeney, and N. F. Roderick, Phys. Plasmas **5**, 4183 (1998).
[29] S. Yu. Gus'kov, G. V. Ivanenkov, A. R. Mingaleev, S. A. Pikuz, T. A. Shelkovenko, and D. A. Hammer, JETP Lett. **67**, 559 (1998).
[30] G. V. Ivanenkov, A. R. Mingaleev, S. A. Pikuz, V. M. Romanova, T. A. Shelkovenko, W. Stepniewski, and D. A. Hammer, JETP **87**, 663 (1998).
[31] S. V. Lebedev, I. H. Mitchell, R. Aliaga-Rossel, S. N. Bland, J. P. Chittenden, A. E. Dangor, and M. G. Haines, Phys. Rev. Lett. **81**, 4152 (1998).
[32] B. M. Marder, T. W. L. Sanford, and G. O. Allshouse, Phys. Plasmas **5**, 2997 (1998).
[33] D. L. Peterson, R. L. Bowers, K. D. McLenithan, C. Deeney, G. A. Chandler, R. B. Spielman, M. K. Matzen, and N. F. Roderick, Phys. Plasmas **5**, 3302 (1998).
[34] R. B. Spielman, C. Deeney, G. A. Chandler, M. R. Douglas, D. L. Fehl, M. K. Matzen, D. H. McDaniel, T. J. Nash, J. L. Porter, T. W. L. Sanford, J. F. Seamen, W. A. Stygar, K. W. Struve, S. P. Breeze, J. S. McGurn, J. A. Torres, D. M. Zagar, T. L. Gilliland, D. O. Jobe, J. L. McKenney, R. C. Mock, M. Vargas, T. Wagoner, and D. L. Peterson, Phys. Plasmas **5**, 2105 (1998).
[35] K. L. Baker, J. L. Porter, L. E. Ruggles, G. A. Chandler, C. Deeney, M. Vargas, A. Moats, K. Struve, J. Torres, J. McGurn, W. W. Simpson, D. L. Fehl, R. E. Chrien, W. Matuska, and G. C. Idzorek, Appl. Phys. Lett. **75**, 775 (1999).
[36] K. L. Baker, J. L. Porter, L. E. Ruggles, R. E. Chrien, and G. C. Idzorek, Rev. Sci. Instrum. **70**, 1624 (1999).
[37] K. L. Baker, J. L. Porter, L. E. Ruggles, D. L. Fehl, G. A. Chandler, M. Vargas, L. P. Mix, W. W. Simpson, Chris Deeney, R. E. Chrien, and G. C. Idzorek, Rev. Sci. Instrum. **70**, 2012 (1999).
[38] R. Benattar, S. V. Zakharov, A. F. Nikiforov, V. G. Novikov, V. A. Gasilov, A. Yu. Krukovskii, and V. S. Zakharov, Phys. Plasmas **6**, 175 (1999).
[39] J. P. Chittenden, S. V. Lebedev, A. R. Bell, R. Aliaga-Rossel, S. N. Bland, and M. G. Haines, Phys. Rev. Lett. **83**, 100 (1999).
[40] C. Deeney, C. A. Coverdale, M. R. Douglas, K. W. Struve, R. B. Spielman, W. A. Stygar, D. L. Peterson, N. F. Roderick, M. G. Haines, F. N. Beg, and J. Ruiz-Camacho, Phys. Plasmas **6**, 3576 (1999).
[41] M. Derzon, T. Nash, G. Chandler, G. Cooper, D. Fehl, C. Hall, J. Lash, R. Leeper, E. McGuire, R. Mock, R. Olson, C. Olson, G. E. Rochau, G. A. Rochau, C. Ruiz, J. Seamen, S. Slutz, W. Stygar, M. A. Sweeney, S. Lazier, D. Droemer, T. Helvin, and R. Starbird, Rev. Sci. Instrum. **70**, 566 (1999).
[42] M. P. Desjarlais and B. M. Marder, Phys. Plasmas **6**, 2057 (1999).
[43] T. A. Golub, N. B. Volkov, R. B. Spielman, and N. A. Gondarenko, Appl. Phys. Lett. **74**, 3624 (1999).
[44] J. H. Hammer, M. Tabak, S. C. Wilks, J. D. Lindl, D. S. Bailey, P. W. Rambo, A. Toor, G. B. Zimmerman, and J. L. Porter, Jr., Phys. Plasmas **6**, 2129 (1999).

[45] J. H. Hammer and D. D. Ryutov, Phys. Plasmas **6**, 3302 (1999).
[46] G. V. Ivanenkov, A. R. Mingaleev, S. A. Pikuz, D. A. Hammer, and T. A. Shelkovenko, Plasma Phys. Rep. **25**, 783 (1999).
[47] S. V. Lebedev, R. Aliaga-Rossel, S. N. Bland, J. P. Chittenden, A. E. Dangor, M. G. Haines, and I. H. Mitchell, Phys. Plasmas **6**, 2016 (1999).
[48] R. J. Leeper *et al.*, Nucl. Fusion **39**, 1283 (1999).
[49] M. A. Liberman, J. S. De Groot, A. Toor, and R. B. Spielman, *Physics of High-Density Z-Pinch Plasmas* (Springer, New York, 1999).
[50] I. V. Lisitsyn, S. Katsuki, and H. Akiyama, Phys. Plasmas **6**, 1389 (1999).
[51] J. J. MacFarlane, M. S. Derzon, T. J. Nash, G. A. Chandler, and D. L. Peterson, Rev. Sci. Instrum. **70**, 323 (1999).
[52] T. J. Nash, M. S. Derzon, G. A. Chandler, R. Leeper, D. Fehl, J. Lash, C. Ruiz, G. Cooper, J. F. Seamen, J. McGurn, S. Lazier, J. Torres, D. Jobe, T. Gilliland, M. Hurst, R. Mock, P. Ryan, D. Nielsen, J. Armijo, J. McKenney, R. Hawn, D. Hebron, J. J. MacFarlane, D. Peterson, R. Bowers, W. Matuska, and D. D. Ryutov, Phys. Plasmas **6**, 2023 (1999).
[53] T. Nash, M. Derzon, R. Leeper, D. Jobe, M. Hurst, and J. Seamen, Rev. Sci. Instrum. **70**, 302 (1999).
[54] T. J. Nash, M. S. Derzon, G. A. Chandler, D. Fehl, R. Leeper, M. Hurst, D. Jobe, J. Torres, J. Seamen, S. Lazier, T. Gilliland, and J. McGurn, Rev. Sci. Instrum. **70**, 464 (1999).
[55] R. E. Olson, G. A. Chandler, M. S. Derzon, D. E. Hebron, J. S. Lash, R. J. Leeper, T. J. Nash, G. E. Rochau, T. W. L. Sanford, N. B. Alexander, and C. R. Gibson, Fusion Technol. **35**, 260 (1999).
[56] D. L. Peterson, R. L. Bowers, W. Matuska, K. D. McLenithan, G. A. Chandler, C. Deeney, M. S. Derzon, M. Douglas, M. K. Matzen, T. J. Nash, R. B. Spielman, K. W. Struve, W. A. Stygar, and N. F. Roderick, Phys. Plasmas **6**, 2178 (1999).
[57] S. A. Pikuz, T. A. Shelkovenko, A. R. Mingaleev, D. A. Hammer, and H. P. Neves, Phys. Plasmas **6**, 4272 (1999).
[58] S. A. Pikuz, T. A. Shelkovenko, D. B. Sinars, J. B. Greenly, Y. S. Dimant, and D. A. Hammer, Phys. Rev. Lett. **83**, 4313 (1999).
[59] G. E. Rochau, M. Derzon, D. Fehl, G. A. Rochau, M. A. Sweeney, D. Tabor, S. E. Lazier, D. Droemer, T. Helvin, and R. Starbird, Rev. Sci. Instrum. **70**, 553 (1999).
[60] J. Ruiz-Camacho, F. N. Beg, A. E. Dangor, M. G. Haines, E. L. Clark, and I. Ross, Phys. Plasmas **6**, 2579 (1999).
[61] T. W. L. Sanford, R. C. Mock, T. J. Nash, K. G. Whitney, P. E. Pulsifer, J. P. Apruzese, D. Mosher, D. L. Peterson, and M. G. Haines, Phys. Plasmas **6**, 1270 (1999).
[62] T. W. L. Sanford, R. C. Mock, R. B. Spielman, M. G. Haines, J. P. Chittenden, K. G. Whitney, J. P. Apruzese, D. L. Peterson, J. B. Greenly, D. B. Sinars, D. B. Reisman, and D. Mosher, Phys. Plasmas **6**, 2030 (1999).
[63] T. W. L. Sanford, R. E. Olson, R. L. Bowers, G. A. Chandler, M. S. Derzon, D. E. Hebron, R. J. Leeper, R. C. Mock, T. J. Nash, D. L. Peterson, L. E. Ruggles, W. W. Simpson, K. W. Struve, and R. A. Vesey, Phys. Rev. Lett. **83**, 5511 (1999).
[64] T. A. Shelkovenko, S. A. Pikuz, A. R. Mingaleev, and D. A. Hammer, Rev. Sci. Instrum. **70**, 667 (1999).
[65] R. E. Terry, J. Davis, C. Deeney, and A. L. Velikovich, Phys. Rev. Lett. **83**, 4305 (1999).
[66] K. G. Whitney, Phys. Plasmas **6**, 816 (1999).
[67] K. L. Baker, J. L. Porter, L. E. Ruggles, G. A. Chandler, C. Deeney, M. Vargas, A. Moats, K. Struve, J. Torres, J. S. McGurn, W. W. Simpson, D. L. Fehl, D. O. Jobe, R. E. Chrien, W. Matuska, and G. C. Idzorek, Phys. Plasmas **7**, 681 (2000).
[68] J. P. Chittenden, S. V. Lebedev, J. Ruiz-Camacho, F. N. Beg, S. N. Bland, C. A. Jennings, A. R. Bell, M. G. Haines, S. A. Pikuz, T. A. Shelkovenko, and D. A. Hammer, Phys. Rev. E **61**, 4370 (2000).
[69] M. R. Douglas, C. Deeney, R. B. Spielman, C. A. Coverdale, N. F. Roderick, and D. L. Peterson, Phys. Plasmas **7**, 1935 (2000).
[70] M. R. Douglas, C. Deeney, R. B. Spielman, C. A. Coverdale, N. F. Roderick, and M. G. Haines, Phys. Plasmas **7**, 2945 (2000).
[71] S. Yu. Gus'kov, G. V. Ivanenkov, A. R. Mingaleev, V. V. Nikishin, S. A. Pikuz, V. B. Rozanov, W. Stepniewski, V. F. Tishkin, D. A. Hammer, and T. A. Shelkovenko, Plasma Phys. Rep. **26**, 745 (2000).
[72] M. G. Haines, S. V. Lebedev, J. P. Chittenden, F. N. Beg, S. N. Bland, and A. E. Dangor, Phys. Plasmas **7**, 1672 (2000).
[73] S. V. Lebedev, R. Aliaga-Rossel, S. N. Bland, J. P. Chittenden, A. E. Dangor, M. G. Haines, and M. Zakaullah, Phys. Rev. Lett. **84**, 1708 (2000).
[74] S. V. Lebedev, F. N. Beg, S. N. Bland, J. P. Chittenden, A. E. Dangor, M. G. Haines, S. A. Pikuz, and T. A. Shelkovenko, Phys. Rev. Lett. **85**, 98 (2000).
[75] L. I. Rudakov, A. L. Velikovich, J. Davis, J. W. Thornhill, J. L. Giuliani, Jr., and C. Deeney, Phys. Rev. Lett. **84**, 3326 (2000).
[76] D. D. Ryutov, M. S. Derzon, and M. K. Matzen, Rev. Mod. Phys. **72**, 167 (2000).
[77] T. W. L. Sanford, R. E. Olson, R. C. Mock, G. A. Chandler, R. J. Leeper, T. J. Nash, L. E. Ruggles, W. W. Simpson, K. W. Struve, D. L. Peterson, R. L. Bowers, and W. Matuska, Phys. Plasmas **7**, 4669 (2000).
[78] T. W. L. Sanford, R. E. Olson, R. A. Vesey, G. A. Chandler, D. E. Hebron, R. C. Mock, R. J. Leeper, T. J. Nash, C. L. Ruiz, L. E. Ruggles, W. W. Simpson, R. L. Bowers, W. Matuska, D. L. Peterson, and R. R. Peterson, Fusion Technol. **38**, 11 (2000).
[79] N. Shimomura, M. Nagata, Y. Teramoto, and H. Akiyama, Jpn. J. Appl. Phys., Part 1 **39**, 6051 (2000).
[80] D. B. Sinars, T. A. Shelkovenko, S. A. Pikuz, Min Hu, V. M. Romanova, K. M. Chandler, J. B. Greenly, D. A. Hammer, and B. R. Kusse, Phys. Plasmas **7**, 429 (2000).
[81] A. L. Velikovich, J. Davis, J. W. Thornhill, J. L. Giuliani, Jr., L. I. Rudakov, and C. Deeney, Phys. Plasmas **7**, 3265 (2000).
[82] K. G. Whitney, Phys. Plasmas **7**, 657 (2000).
[83] J. P. Apruzese, J. W. Thornhill, K. G. Whitney, J. Davis, C. Deeney, and C. A. Coverdale, Phys. Plasmas **8**, 3799 (2001).
[84] R. B. Baksht, A. Yu. Labetsky, A. G. Rousskikh, A. V. Fedyunin, A. V. Shishlov, V. A. Kokshenev, N. E. Kurmaev, and F. I. Fursov, Plasma Phys. Rep. **27**, 557 (2001).
[85] J. P. Chittenden, S. V. Lebedev, S. N. Bland, A. Ciardi, and M. G. Haines, Phys. Plasmas **8**, 675 (2001).

[86] J. P. Chittenden, S. V. Lebedev, S. N. Bland, F. N. Beg, and M. G. Haines, Phys. Plasmas **8**, 2305 (2001).
[87] M. E. Cuneo, R. A. Vesey, J. H. Hammer, J. L. Porter, Jr., L. E. Ruggles, and W. W. Simpson, Laser Part. Beams **19**, 481 (2001).
[88] M. E. Cuneo, R. A. Vesey, J. L. Porter, Jr., G. A. Chandler, D. L. Fehl, T. L. Gilliland, D. L. Hanson, J. S. McGurn, P. G. Reynolds, L. E. Ruggles, H. Seamen, R. B. Spielman, K. W. Struve, W. A. Stygar, W. W. Simpson, J. A. Torres, D. F. Wenger, J. H. Hammer, P. W. Rambo, D. L. Peterson, and G. C. Idzorek, Phys. Plasmas **8**, 2257 (2001).
[89] M. R. Douglas, C. Deeney, and N. F. Roderick, Phys. Plasmas **8**, 238 (2001).
[90] R. F. Heeter, J. E. Bailey, M. E. Cuneo, J. Emig, M. E. Foord, P. T. Springer, and R. S. Thoe, Rev. Sci. Instrum. **72**, 1224 (2001).
[91] S. V. Lebedev, F. N. Beg, S. N. Bland, J. P. Chittenden, A. E. Dangor, M. G. Haines, K. H. Kwek, S. A. Pikuz, and T. A. Shelkovenko, Phys. Plasmas **8**, 3734 (2001).
[92] S. V. Lebedev, F. N. Beg, S. N. Bland, J. P. Chittenden, A. E. Dangor, M. G. Haines, M. Zakaullah, S. A. Pikuz, T. A. Shelkovenko, and D. A. Hammer, Rev. Sci. Instrum. **72**, 671 (2001).
[93] J. J. MacFarlane, J. E. Bailey, T. A. Mehlhorn, G. A. Chandler, T. J. Nash, C. Deeney, and M. R. Douglas, Rev. Sci. Instrum. **72**, 1228 (2001).
[94] T. J. Nash *et al.*, Rev. Sci. Instrum. **72**, 1167 (2001).
[95] R. E. Olson, T. W. L. Sanford, G. A. Chandler, R. J. Leeper, R. C. Mock, J. S. McGurn, S. E. Lazier, J. C. Armijo, S. Dropinski, L. E. Ruggles, W. W. Simpson, J. A. Torres, and C. Wakefield, Rev. Sci. Instrum. **72**, 1214 (2001).
[96] T. W. L. Sanford, Laser Part. Beams **19**, 541 (2001).
[97] T. W. L. Sanford, J. E. Bailey, G. A. Chandler, M. E. Cuneo, D. L. Fehl, D. E. Hebron, R. J. Leeper, R. W. Lemke, R. C. Mock, R. E. Olson, T. J. Nash, J. L. Porter, L. E. Ruggles, C. L. Ruiz, W. W. Simpson, K. W. Struve, W. A. Stygar, R. L. Bowers, R. E. Chrien, G. C. Idzorek, W. Matuska, D. L. Peterson, and R. G. Watt, Rev. Sci. Instrum. **72**, 1217 (2001).
[98] G. S. Sarkisov, B. S. Bauer, and J. S. De Groot, JETP Lett. **73**, 69 (2001).
[99] D. B. Sinars, Min Hu, K. M. Chandler, T. A. Shelkovenko, S. A. Pikuz, J. B. Greenly, D. A. Hammer, and B. R. Kusse, Phys. Plasmas **8**, 216 (2001).
[100] S. A. Slutz, M. R. Douglas, J. S. Lash, R. A. Vesey, G. A. Chandler, T. J. Nash, and M. S. Derzon, Phys. Plasmas **8**, 1673 (2001).
[101] R. B. Spielman and J. S. De Groot, Laser Part. Beams **19**, 509 (2001).
[102] W. A. Stygar, R. E. Olson, R. B. Spielman, and R. J. Leeper, Phys. Rev. E **64**, 026410 (2001).
[103] J. W. Thornhill, J. P. Apruzese, J. Davis, R. W. Clark, A. L. Velikovich, J. L. Giuliani, Jr., Y. K. Chong, K. G. Whitney, C. Deeney, C. A. Coverdale, and F. L. Cochran, Phys. Plasmas **8**, 3480 (2001).
[104] A. L. Velikovich, K. G. Whitney, and J. W. Thornhill, Phys. Plasmas **8**, 4524 (2001).
[105] K. G. Whitney, P. E. Pulsifer, J. P. Apruzese, J. W. Thornhill, J. Davis, Y. K. Chong, T. W. L. Sanford, R. C. Mock, and T. J. Nash, Phys. Plasmas **8**, 3708 (2001).
[106] J. P. Apruzese, J. Davis, K. G. Whitney, J. W. Thornhill, P. C. Kepple, R. W. Clark, C. Deeney, C. A. Coverdale, and T. W. L. Sanford, Phys. Plasmas **9**, 2411 (2002).
[107] J. E. Bailey, G. A. Chandler, D. Cohen, M. E. Cuneo, M. E. Foord, R. F. Heeter, D. Jobe, P. W. Lake, J. J. MacFarlane, T. J. Nash, D. S. Nielsen, R. Smelser, and J. Torres, Phys. Plasmas **9**, 2186 (2002).
[108] J. E. Bailey, G. A. Chandler, S. A. Slutz, G. R. Bennett, G. Cooper, J. S. Lash, S. Lazier, R. Lemke, T. J. Nash, D. S. Nielsen, T. C. Moore, C. L. Ruiz, D. G. Schroen, R. Smelser, J. Torres, and R. A. Vesey, Phys. Rev. Lett. **89**, 095004 (2002).
[109] F. N. Beg, S. V. Lebedev, S. N. Bland, J. P. Chittenden, A. E. Dangor, and M. G. Haines, Phys. Plasmas **9**, 375 (2002).
[110] G. R. Bennett, M. E. Cuneo, R. A. Vesey, J. L. Porter, R. G. Adams, R. A. Aragon, J. A. Caird, O. L. Landen, P. K. Rambo, D. C. Rovang, L. E. Ruggles, W. W. Simpson, I. C. Smith, and D. F. Wenger, Phys. Rev. Lett. **89**, 245002 (2002).
[111] M. E. Cuneo, R. A. Vesey, J. L. Porter, Jr., G. R. Bennett, D. L. Hanson, L. E. Ruggles, W. W. Simpson, G. C. Idzorek, W. A. Stygar, J. H. Hammer, J. J. Seamen, J. A. Torres, J. S. McGurn, and R. M. Green, Phys. Rev. Lett. **88**, 215004 (2002).
[112] D. L. Hanson, R. A. Vesey, M. E. Cuneo, J. L. Porter, Jr., G. A. Chandler, L. E. Ruggles, W. W. Simpson, J. Torres, J. McGurn, D. Hebron, S. C. Dropinski, J. H. Hammer, G. R. Bennett, H. Seamen, T. L. Gilliland, and D. G. Schroen, Phys. Plasmas **9**, 2173 (2002).
[113] S. V. Lebedev, F. N. Beg, S. N. Bland, J. P. Chittenden, A. E. Dangor, and M. G. Haines, Phys. Plasmas **9**, 2293 (2002).
[114] T. W. L. Sanford, R. W. Lemke, R. C. Mock, G. A. Chandler, R. J. Leeper, C. L. Ruiz, D. L. Peterson, R. E. Chrien, G. C. Idzorek, R. G. Watt, and J. P. Chittenden, Phys. Plasmas **9**, 3573 (2002).
[115] T. W. L. Sanford, N. F. Roderick, R. C. Mock, K. W. Struve, and D. L. Peterson, IEEE Trans. Plasma Sci. **30**, 538 (2002).
[116] G. S. Sarkisov, P. V. Sasorov, K. W. Struve, D. H. McDaniel, A. N. Gribov, and G. M. Oleinik, Phys. Rev. E **66**, 046413 (2002).
[117] A. L. Velikovich, I. V. Sokolov, and A. A. Esaulov, Phys. Plasmas **9**, 1366 (2002).
[118] R. A. Vesey, M. E. Cuneo, G. R. Bennett, J. L. Porter, Jr., R. G. Adams, R. A. Aragon, P. K. Rambo, L. E. Ruggles, W. W. Simpson, and I. C. Smith, Phys. Rev. Lett. **90**, 035005 (2003).
[119] R. B. Spielman *et al.*, in *Proceedings of the 11th IEEE International Pulsed Power Conference*, edited by G. Cooperstein and I. Vitkovitsky (IEEE, Baltimore, 1997), p. 709.
[120] P. A. Corcoran *et al.*, in *Proceedings of the 11th IEEE International Pulsed Power Conference* [119], p. 466.
[121] R. J. Garcia *et al.*, in *Proceedings of the 11th IEEE International Pulsed Power Conference* [119], p. 1614.
[122] H. C. Ives *et al.*, in *Proceedings of the 11th IEEE International Pulsed Power Conference* [119], p. 1602.
[123] M. A. Mostrom *et al.*, in *Proceedings of the 11th IEEE International Pulsed Power Conference* [119], p. 460.
[124] R. W. Shoup *et al.*, in *Proceedings of the 11th IEEE International Pulsed Power Conference* [119], p. 1608.
[125] I. D. Smith *et al.*, in *Proceedings of the 11th IEEE Interna-*

tional Pulsed Power Conference [119], p. 168.
[126] K. W. Struve *et al.*, in *Proceedings of the 11th IEEE International Pulsed Power Conference* [119], p. 162.
[127] W. A. Stygar *et al.*, in *Proceedings of the 11th IEEE International Pulsed Power Conference* [119], p. 591.
[128] K. W. Struve, J. P. Corley, D. L. Johnson, D. H. McDaniel, R. B. Spielman, and W. A. Stygar, *Proceedings of the 12th IEEE International Pulsed Power Conference*, edited by C. Stallings and H. Kirbie (IEEE, Monterey, CA, 1999), p. 493.
[129] D. H. McDaniel, M. G. Mazarakis, D. E. Bliss, J. M. Elizondo, H. C. Harjes, H. C. Ives III, D. L. Kitterman, J. E. Maenchen, T. D. Pointon, S. E. Rosenthal, D. L. Smith, K. W. Struve, W. A. Stygar, E. A. Weinbrecht, D. L. Johnson, and J. P. Corley, in *Dense Z Pinches*, edited by J. Davis, C. Deeney, and N. R. Pereira, AIP Conf. Proc. No. 651 (AIP, Melville, NY, 2002), p. 23.
[130] C. Deeney and R. B. Spielman (unpublished).
[131] M. L. Horry, J. P. Corley, J. A. Mills, and H. D. McGovern (private communication).
[132] M. E. Cuneo, G. A. Chandler, R. A. Vesey, J. L. Porter, T. J. Nash, J. E. Bailey, R. A. Aragon, W. E. Fowler, W. A. Stygar, K. W. Struve, J. A. Torres, J. S. McGurn, S. E. Lazier, D. S. Nielsen, J. P. Chittenden, and S. V. Lebedev, Bull. Am. Phys. Soc. **46**, 234 (2001).
[133] G. A. Chandler, C. Deeney, M. Cuneo, D. L. Fehl, J. S. McGurn, R. B. Spielman, J. A. Torres, J. L. McKenney, J. Mills, and K. W. Struve, Rev. Sci. Instrum. **70**, 561 (1999).
[134] R. B. Spielman, C. Deeney, D. L. Fehl, D. L. Hanson, N. R. Keltner, J. S. McGurn, and J. L. McKenney, Rev. Sci. Instrum. **70**, 651 (1999).
[135] D. L. Fehl, D. J. Muron, R. J. Leeper, G. A. Chandler, C. Deeney, W. A. Stygar, and R. B. Spielman, Rev. Sci. Instrum. **70**, 270 (1999).
[136] L. E. Ruggles, R. B. Spielman, J. L. Porter, Jr., and S. P. Breeze, Rev. Sci. Instrum. **66**, 712 (1995).
[137] L. E. Ruggles, J. L. Porter, W. W. Simpson, and M. F. Vargas, Rev. Sci. Instrum. **70**, 646 (1999).
[138] D. L. Fehl (unpublished).
[139] W. A. Stygar *et al.*, in *Proceedings of the 11th IEEE International Pulsed Power Conference* [119], p. 1258.
[140] T. P. Hughes and R. E. Clark (unpublished).
[141] T. P. Hughes and R. E. Clark (unpublished).
[142] T. D. Pointon, W. A. Stygar, R. B. Spielman, H. C. Ives, and K. W. Struve, Phys. Plasmas **8**, 4534 (2001).
[143] T. P. Hughes, R. E. Clark, B. V. Oliver, R. A. St. John, and W. A. Stygar (unpublished).
[144] Ya. B. Zel'dovich and Yu. P. Raizer, *Physics of Shock Waves and High-Temperature Hydrodynamic Phenomena* (Academic Press, New York, 1966), Vol. I.
[145] J. D. Lindl, *Inertial Confinement Fusion* (Springer-Verlag, New York, 1998), p. 87.
[146] M. E. Cuneo (unpublished).
[147] N. A. Bobrova, T. L. Razinkova, and P. V. Sasarov, Sov. J. Plasma Phys. **18**, 269 (1992).
[148] C. A. Coverdale, C. Deeney, M. R. Douglas, J. P. Apruzese, K. G. Whitney, J. W. Thornhill, and J. Davis, Phys. Rev. Lett. **88**, 065001 (2002).
[149] M. Mazarakis, M. Douglas, M. Cuneo, G. Chandler, T. Nash, and W. Stygar, Bull. Am. Phys. Soc. **46**, 27 (2001).
[150] M. G. Mazarakis, M. R. Douglas, C. E. Deeney, W. A. Stygar, T. J. Nash, M. E. Cuneo, and G. A. Chandler, in *Proceedings of the 29th IEEE International Conference on Plasma Science*, IEEE Catalog No. 02CH37340, edited by IEEE (IEEE, Banff, Canada, 2002), p. 105.
[151] M. Mazarakis, C. Deeney, W. Stygar, T. Nash, M. Cuneo, G. Chandler, and M. Douglas, Bull. Am. Phys. Soc. **47**, 189 (2002).
[152] D. H. McDaniel (unpublished).
[153] R. B. Spielman (unpublished).
[154] J. Topping, *Errors of Observation and Their Treatment* (Chapman and Hall, London, 1972).
[155] J. R. Taylor, *An Introduction to Error Analysis* (University Science, Sausalito, CA, 1997).
[156] *Handbook of Mathematical Functions*, edited by Milton Abramowitz and Irene A. Stegun (Dover, New York, 1972).
[157] D. L. Peterson, R. L. Bowers, J. H. Brownell, A. E. Greene, K. D. McLenithan, T. A. Oliphant, N. F. Roderick, and A. J. Scannapieco, Phys. Plasmas **3**, 368 (1996).
[158] W. Matuska, R. L. Bowers, J. H. Brownell, H. Lee, C. M. Lund, D. L. Peterson, and N. F. Roderick, Phys. Plasmas **3**, 1415 (1996).
[159] P. Coullet, C. Elphick, and D. Repaux, Phys. Rev. Lett. **58**, 431 (1987).
[160] S. Ciliberto and M. Caponeri, Phys. Rev. Lett. **64**, 2775 (1990).
[161] M. C. Cross and P. C. Hohenberg, Rev. Mod. Phys. **65**, 851 (1993).
[162] H. Xi and J. D. Gunton, Phys. Rev. E **52**, 4963 (1995).